Tribological Performance of Ferritic Nitrocarburizing (FNC) Treated Automotive Brake Discs

Chandan Kumar Ravindra Reddy **Shanmukharaj Jayasankar**

2021

CODEN: LUTMDN/(TMMV-5315)/1-76/2021

LUND UNIVERSITY

LTH

FACULTY OF ENGINEERING

MASTER THESIS
DIVISION OF PRODUCTION AND MATERIALS ENGINEERING
LUND UNIVERSITY

Supervisor: Jens Wahlström
Co Supervisor: Oleksandr Gutnichenko
Co Supervisor: Rebecka Lindvall
Industrial Supervisor: Samuel Awe, Automotive Components Floby AB
Examiner: Jan-Eric Ståhl, Professor.

Author: Chandan Kumar Ravindra Reddy and Shanmukaraj Jayasankar
Lund, Sweden 2021

Avdelningen för Industriell Produktion
Lunds Tekniska Högskola
Lunds universitet
Box 118
221 00 Lund
Sverige

Division of Production and Materials Engineering
LTH, School of Engineering
Lund University
Box 118
SE-221 00 Lund
Sweden

Printed in Sweden
Media-Tryck
Lund University

Foreword

We would like to express our sincere gratitude and thanks towards our Supervisor Jens Wahlström Professor, Chair of Machine Elements Lund University (LTH), Department of Mechanical Engineering Division of Machine Elements Lund University, for his guidance, invaluable inspiration, words of advice, and unstinted support throughout the thesis work.

Our sincere thanks to Samuel Awe, Automotive Components Floby AB for his encouragement, suggestions, and support throughout the thesis work.

Our sincere thanks to Oleksandr Gutnichenko, Department of Mechanical Technology, Industrial production and Rebecka Lindvall Ph.D. student Faculty of Engineering, Department of Mechanical Engineering, Division of Production and Materials Engineering, Lund University for their support, encouragement and providing valuable suggestions and helping us out to perform the laboratory work during project works.

We are thankful to our parents for their blessings, moral support, encouragement that has enabled us to complete the thesis work successfully. We thank all our friends who have been our backbone and relatives for their constant motivation and support.

Before concluding, we wholeheartedly thank all the Department, Production and Materials Engineering, Lund University, and those who have directly & indirectly motivated us by giving their precious time and advice.

Lund 2021-06-02

Chandan Kumar Ravindra Reddy & Shanmukaraj Jayasankar

Abstract

The increase of electric vehicles in the market demands the automotive industries to search for better brake disc material with high wear resistance, corrosion resistance, and longer service life. The GCI brake discs, a traditionally used material that has less wear and corrosion resistance. So, the innovative solution to overcome the problem is Ferritic Nitrocarburizing (FNC) treatment on the GCI brake disc. The study aims to investigate the tribological behavior of the FNC-treated and untreated GCI brake discs. The three brake discs used for this study are i) Gray Cast Iron (GCI), ii) Ferritic NitroCarburized (FNC) treated GCI, and iii) Post oxidized FNC treated GCI (Corr-I-Durr) brake discs. The brake pads used in all these experiments are of Non-Asbestos Origin (NAO) material. A tribotester machine was used to investigate the tribological behavior of the brake discs, and information about the Coefficient of Friction (COF) and wear of the discs was obtained. The samples were prepared and etched to analyze the microstructures using the Scanning Electron Microscope (SEM) and Optical Microscope. The Microhardness of the brake discs is measured using the Vickers Hardness indentor. The study shows how the COF and Wear vary for different contact pressure and sliding velocities for the FNC-treated and untreated brake discs, and graphs are plotted. The COF and wear rate are influenced by the surface roughness, hardness, thickness of the compound layer, and the microstructure of the brake disc material. The compound layer which is formed during the FNC process will influence the performance of the brake discs. FNC-treated brake discs show high COF and high wear rate compared to the untreated GCI brake discs.

Keywords: Tribology, GCI, FNC, COF, Wear.

Table of Content

List of Figures

List of Tables

List of Symbols

Symbol	Description	Unit
P	Pressure	Mpa
V	Velocity	m/s
HV.	Hardness Value	-
T	Temperature	°C
F	Force	N
F_t	Tangential Force	N
F_n	Normal Force	N
µ	Coefficient of friction	-
D	Diameter	mm
Ra	Roughness Average	µm
Rz	Average maximum Height of the Profile	µm
Rmax	Maximum Roughness Depth	µm
L_t	Length	mm
Δm	Mass loss	g
ρ	Density	g/cm^3
s	Sliding distance	m

1. Introduction

1.1. Project Background

In recent years, the automobile industry has experienced rapid growth. In every aspect, the automobile industries are working to make the betterment of their product. Brake systems are a common feature of aircraft, cars, cranes, wind turbines, and other mechanical machinery. The brake disc and brake pads are essential components in the braking system that are mainly used to decelerate or stop moving vehicles. A caliper with a piston, a rotor, and two pads make up a typical disc brake unit. Friction brakes operate on the theory that friction pads are pushed against the rotating disc resulting in frictional forces that slows the rotating vehicle wheel. As a result of this, the vehicle's speed is minimized or stopped [1]. To avoid brake fade, the brake disc must have high thermal resistance, a stable COF, and wear uniformly during its service life [2].

The GCI material has been traditionally used in the production of automotive brake discs for decades. The automotive industry wants to be more sustainable and produce products with good corrosion resistance, long lifespan, and good wear resistance due to increasing government regulation on emission. There are two types of emission, which are exhaust emission and non-exhaust emission. Exhaust emissions have been significantly reduced in recent years, and still, the automobile industries are working on it. But non-exhaust emissions like tire wear, road abrasion, and brake wear produce a particulate matter (PM) on the micrometer scale, which becomes airborne in the debris of worn material surfaces, posing a threat to human health and the environment. The brake disc and brake pad wear are all sources of PMs [3]. The World Health Organization (WHO) and European Union (EU) have given air pollution a lot of attention over the last few decades, which was more concentrated on exhaust emission, but now they are looking to the non-exhaust emission as the PMs can have an adverse effect on human health and the environment. PMs emissions from vehicle brake wear would almost certainly push the automotive industry to look for different ways to reduce or eliminate particle emissions.

The introduction of a hybrid vehicle and Electric Vehicles (EVs) is another factor that will boost the global automotive-market. EV uses regenerative braking. In regenerative braking, the kinetic energy produced by the wheel is converted to electrical energy, and it is stored in the motor during braking, deceleration, or downhill running [4]. Regenerative braking is always not enough when there is a need for emergency braking to stop the vehicle, so there is a combination with friction braking to get enough braking power to stop the vehicle. Since the friction brakes are used less or occasionally in the EVs, and the brake disc rotors made of the GCI, will lead to high corrosion and wear problems in the EVs [5].

1.2. Problem Statement

GCI brake discs have poor corrosion resistance and wear performance; they are a great concern to the automotive industry. It is believed that GCI brake discs have more wear rate, and now the EU government is making strict regulations on particle emissions, so the automobile makers are trying to find out to solving this challenge before it becomes an issue. The one solution is nitrocarburizing the GCI disc surface. But the effect of this treatment on the tribological behavior of the discs is not investigated yet.

1.3. Project Purpose

This project aims to determine FNC treated GCI brake disc's tribological behavior, which is considered to show high wear resistance and corrosion resistance compared to the untreated GCI brake disc. This is to understand how the FNC treated GCI brake disc results when the tribotest is performed compared to the untreated GCI brake disc. The vehicle braking performance is dependent on the tribological properties of the brake disc and brake pads. The aim is to understand the alternative solution that can be implemented. So that we can replace it with the GCI brake disc in the EVs in upcoming years. To incorporate these solutions, it is necessary to understand better and define their viability and potential failure factors.

1.4. Research question

Research questions were framed to make the authors focus on what direction the research should be carried out.

RQ1) What is the effect of sliding velocity and contact pressure on COF for FNC treated and untreated brake discs?

RQ2) What is the effect of sliding velocity and contact pressure on wear for the FNC treated and untreated brake discs?

1.5. Delimitations

There were some delimitations made in this research. The tests were performed to the maximum values of the tribotester, which were not up to the real-life situations. Only a limited number of workpieces were able to be analysed with the disc brake available.

1.6. Structure of the thesis

The thesis structure is divided into seven individual chapters. Chapter 2 discusses the research framework and how the methodology is selected. Chapter 3 explains the theoretical background, including the overview of the brake discs and detailed explanation of the FNC process. Chapter 4 explains the experimental methods and machines are used to perform the experiments. Chapter 5 presents the results that are obtained from the experimentation and analysis. Chapter 6 shows the discussions made from the obtained results. Chapter 7 presents the overall answers to the research questions, and suggestions for future research are concluded.

2. Research Methodology

This chapter explains the approach and the methodology that followed in this project. This chapter also explains the reason why the author had chosen the particular methodology. The later part of the chapter discusses the literature review, data collection methods, and the research quality.

2.1. Research approach

This research follows an exploratory one. Exploratory research is conducted to investigate the problem, which is not clearly defined. This research is conducted to understand the existing problem better. In exploratory research, the researcher will change their direction to the revelation of new data or insights [6]. So, in this thesis work, the phenomenon is to understand the tribological behavior of the FNC surface-treated GCI brake discs. The effect of tribological behavior on FNC-treated Gray Cast Iron brake discs has not been studied yet.

This master thesis is based on the action research methodology by considering the characteristics of the action research and the experiment in which the thesis is carrying out. "Action research is defined as research in action rather than research about action" [7]. Action research follows a scientific approach to study the phenomena with those who experience these problems directly. And action research is participative; in other words, it can explain the researcher's participation and client collaboration to solve the organizational problem and develop knowledge that is useful for both researchers and the industry members [7] [8]. Action research is fundamentally about planning and implementing change in an organization. In this thesis work, the tribological behavior of FNC-treated GCI brake discs is investigated. In this project, the authors collaborated with the client to plan, conduct experiments, evaluate the actions, and further plan moving into other phases.

2.2. Literature Review

This part explains the methodology followed in conducting the literature review to insights into Ferritic Nitrocarburized surface treatment. A literature review will help identify the research questions and helps to build an

understanding of the theoretical concepts and terminology [9]. In this work, the authors conducted an academic literature review. The primary motivation for conducting the academic literature was that the previous research was focused on the Surface treatment of Ferritic Nitrocarburizing on GCI brake discs but did not evaluate the tribological behavior of the brake discs. Hence the authors did the literature review to analyze the brake discs, coatings used so far in the brakes, the need for FNC, Ferritic Nitrocarburized surface treatment, the process of FNC, and their properties.

2.3. Academic Literature

The academic literature review was conducted by searching the journals using the LUB search and Web of Science database, the digital library of Lund University. The works of literature are collected from the publications like Elsevier, Science Direct, Research Gate, and Springer. So we considered these libraries are helpful to gather information regarding the field of study. We started our search using specific keywords like *'Microstructure of GCI, Process of FNC treatment, Tribological performance, COF, Wear.'* Then we narrowed our search by selecting the journals published between the year 2000-2020. After finding the necessary articles, the authors reviewed the problem foundation and the findings.

So apart from the LUB search and Web of Science, we also used other databases like Google to identify the non-academic literature. This search helped us identify the wide variety of articles related to the research topic supporting the academic literature. In this present thesis work, we need to compare the tribological performance of GCI and FNC treated brake discs, a relatively new study. These searches helped us by providing a lot of insights about the topic.

So, this academic literature review helped the authors to gain an initial understanding of the research topic and build the theoretical concepts.

2.4. Data Collection

Data collection gathers information on the variables of interest by the systematic approach to answer the stated research question. The authors used the direct observation method in collecting the data. Direct observation is a qualitative method of data collection and takes a lot of time in which the

researchers must record any potentially useful data accurately for analysis [10].

2.5. Experimental Tests and Observation

The data gathering through structured observation and field tests contributes more reliability and ensures valid data to make it easier to achieve the project objectives. So in the present thesis, 18 tests were carried out using tribotester. The data was recorded using field notes, excel, and photographs. The authors recorded data done in a structured way that involves the information of units to be observed and the information to be recorded.

2.6. Experimental Testing Process

Automotive Components Floby supplied the materials used in this study. The materials include three different GCI discs – two of these discs had been surface treated using the FNC technique while the third disc was untreated and a pair of the NAO brake pad. The authors carried out six different tests on each brake discs material for 100 passes. The authors performed tests with three various forces for two different velocities. Since we have the soft braking and hard braking in the actual scenario, the authors considered the three pressure values: 0.75 MPa, 1.5 MPa, 2.5 MPa, and different velocities of 0.1m/s and 0.3m/s. The conditions are limited due to the specifications of the tribotester and the number of workpieces. By this test condition, the authors analyzed the wear loss and Coefficient of Friction (COF).

Table 1: *Test matrix indicates different pressures and Different velocities and the number of passes being performed.*

Test Condition	P_1=0.75 MPa	P_2=1.5 MPa	P_3=2.5 MPa
V_1=0.1m/s	100 Pass	100 Pass	100 Pass
V_2=0.3m/s	100 Pass	100 Pass	100 Pass

Apart from the tribology experiment, the authors also performed Infocus optical microscope and Tescan Scanning Electron Microscope (SEM) to

analyze the microstructure of the three different samples, and the data was recorded as photographs. Also, the surface roughness and the brake disc's surface hardness were recorded using the field notes. So the detailed experiment setup is explained in chapter 4.

2.7. Research Quality

Action research does not need to justify itself in relation to alternative research approaches. Its own terms can justify action research, and the other research alternatives do not readily capture the reflection, data generation, and theory building [7]. Action researchers should be conscious of theory building, developing the own test assumptions, and testing data to maintain the validity of the research. The main threat to the validity of action research is the lack of impartiality on the researcher's part. "Action researchers are engaged in shaping the story; they need to consider to the extent that the story has a valid presentation on what has taken place and how it is understood by the readers, rather than a biased version" [7]. The four parts of speech suggested by Fisher and Tobert as follows

- Framing – Stating the purpose of speaking about the present occasion and explaining what the researcher is trying to resolve.
- Advocating – Explaining the goal of the research, asserting, and the proposal for action.
- Illustrating – Building up the theory will make the advocacy concrete and orients the others more clearly.
- Inquiring – Questioning the participants to know what they understand and their views.

Action researchers should combine advocacy with the inquiry to present their interferences, views, and opinions as open to testing and evaluation [7]. In this work, the authors have explained what they are trying to resolve and advocate the research's goal and their viewpoints that are open for further research.

2.8. Chapter Summary

The chapter started with an explanation of the research methodology followed in the present work. The second part of the chapter discusses the literature review and the search strategy followed in collecting the literature. The next part of the chapter explains the data collection method and how the

data gathered is reliable. The chapter ends with the quality of the action research and threats in the study, relating the present thesis work with the part of the speech.

3. Theoretical Background

This chapter deals with the theoretical background of the project. The first part of the chapter is about brake discs and the different coatings used. The second part presents the principles Ferritic Nitrocarburizing principles.

3.1. Overview of Brakes

The brake system in the vehicle is to stop or adjust the speed by applying pressure to the brake pads against the rotor. The basic principle in braking is converting kinetic energy into heat energy. In frictional braking, the kinetic energy is converted into thermal energy, while in regenerative braking, it is converted into electric energy. The two types of frictional braking are drum brakes and disc brakes. Brake discs are crucial automotive components that stop the vehicle's motion by converting the kinetic energy into thermal energy, so there will be an increase in temperature due to the friction between the surfaces of brake discs and brake pads [5]. The general overview of the brake disc assembly with a single-piston is shown in Figure 1.

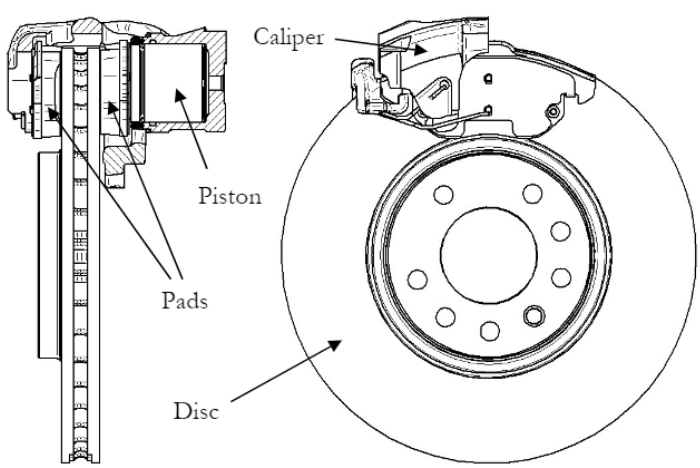

Figure 1: *Disc brake assembly with a single-piston floating caliper and a ventilated disc [11]*

3.1.1. Brake Disc

The brake discs are usually made of GCI material produced through a sand casting process. GCI is the most widely used brake disc material in automobiles because it has excellent friction properties, is inexpensive, maintains strength at high temperatures, is relatively easy to produce, and is thermally stable [1]. The GCI discs have a graphite content that enhances the thermal conductivity, and their huge heat storage ability prevents brake rotors from overheating and brake fades during use. Additives including chromium and molybdenum increase abrasion resistance and improve heat cracking resistance [2]. The hardness of GCI ranges from 200HV to 230HV. The GCI has the advantage of being easily machinability, and castability and the service life of the brake disc is 10^5 kilometers [2]. For these reasons, the GCI material is used as a choice for passenger vehicles.

The GCI has a low corrosion resistance when exposed to increased atmospheric humidity and road salt. Because of corrosion, the red oxide layer on the braking surface can be easily separated, reducing the braking efficiency and shortening the brake disc life [12]. The dust particles produced during braking include PMs of different sizes, which can harm the environment and human health [13]. The coatings or surface treatment is done to GCI to increase corrosion resistance and reduce the wear particle size.

Figure 2 represents a cross-section of a coated or treated disc. The body of the brake discs consists of three layers; one is axial friction (layer 3), an anti-corrosion (layer 4), which is applied over the friction layer, and an anti-abrasion (layer 5), spread over the anti-corrosion layer. The anti-corrosion layer was applied using the plasma powder deposition method or laser deposition welding method. An anti-corrosion layer based on iron has chromium content over 18% to 30%, nickel content over 2% to 8%, and molybdenum over 4.5%. An anti-corrosion layer is also based on carbide reinforcement. The anti-abrasion layer was applied using a thermal spray powder containing SiC with a metal binder. SiC is popularly known for its abrasion resistance to wear; the brake discs coated with SiC significantly show less wear. Outside Europe, manufacturers use NAO friction materials for brake linings [14]. GCI has poor resistance to corrosion and wear, so surface treatment or coatings are required for better performance and longer life of brake discs.

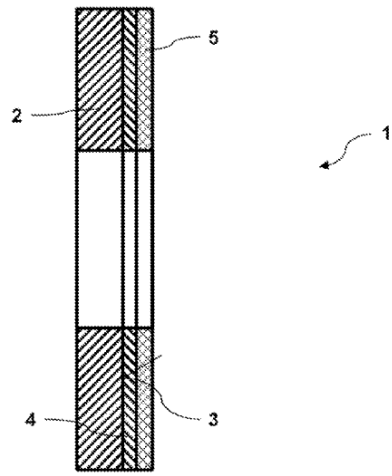

Figure 2: *Cross-section of coated or treated disc 3.Friction layer, 4. Anti-Corrosion layer, 5. Anti-abrasion layer [14]*

3.1.2. Coating Materials

The following section summarizes the material used for coatings deposited on the surface of Gray Cast Iron by either thermal spray deposition methods or laser deposition methods for wear and corrosion resistance. The materials are categorized into three groups as i) oxides, ii) carbides, and iii) other alternative materials.

3.1.2.1. Oxides

Chromium Oxide (Cr_2O_3), Aluminum Oxide (Al_2O_3), Titanium oxide (TiO_2) are used as coating materials because of their resistance to wear and corrosion, and high hardness. These oxides are applied over the GCI by thermal spray techniques at a controlled temperature [4] [15] [16]. These thermally sprayed oxide coatings form the compact triboflim and show favorable properties like wear rate, friction coefficient, etc.

3.1.2.2. Carbides

Tungsten Carbide (WC) and chromium carbide (Cr_3C_2) binded with metals consisting of Cobalt (Co), Nickel (Ni), Chromium (Cr), Iron (Fe) are frequently used carbides for the wear resistance of Gray Cast Iron. The High-velocity thermal spray process applies these carbides. The thermally sprayed cermet carbides are used to resist wear due to their properties abrasion, sliding, and erosion resistance [4] [17] [18] [19]. The performance of the tungsten carbide is due to the size, shape, and distribution of the carbide particles and solution of the carbon in the cobalt matrix. The large volume fraction of tungsten monocarbide in the carbide coating will increase the wear properties of Gray Cast Iron [17]. So, among the hard carbides WC-12Co, WC-10Co-4Cr is the high wear resistance carbide coatings [4].

3.1.2.3. Alternate Materials

The price of Ni and Co were increased there is a need for an alternate material that can resist wear and improve the lifetime of the brake discs. Also, the materials like Ni, Co, and WC-Co-based powders release acceptable wear debris when used as coating materials. The researchers are moved towards the environmentally friendly alternative material or use the material's reduced [20].

The studies show that alloys like Ni-Cr-B-Si with Fe matrix and Fe-V-Cr-C alloy show promising results in improving the wear resistance and tribological properties. The alloys coating with Fe yield better results and will be the possible alternative to Ni-Co-based coatings. Also, they have a lower environmental impact due to the reduced content and lower cost [21] [22].

3.2. The need for nitrocarburizing

The GCI is poor resistant to corrosion and wear. Therefore various surface treatment procedures are developed to overcome these disadvantages. When the GCI brake discs are coated with carbides or oxides, it is added on the top surface and not diffused in the material surface, so these coatings are more susceptible to pitting, flaking, and peeling from the surface [23]. The brake

discs coated with carbides will protect the parts from corrosion and wear, but these coatings are not a permanent solution, as there are many chances of peeling when it subjects to abrasive wear. When the coated surface peels off, the brake pads will directly contact the GCI surface, decreasing the performance of the brakes. So, the peeled-off part either needs to be scrapped or recoated. This process consumes a long time and is expensive. A ferritic low-temperature nitrocarburizing method will be an alternative for coatings. In FNC, the nitrogen will be diffused into the material surface and form the compound layer, which acts as a protective zone and resists wear and corrosion [23]. These nitrided layers diffused into the surface will last for 10000 km for just the thickness layer is 10 µm [14]. So if the thickness of nitride layers is increased, it will last for a long time. And resulting in less chance of flaking and peeling the surface reduces the need for recoating [23].

3.2.1. Ferritic Nitrocarburizing (FNC)

NitroCarburizing is a surface treatment process similar to nitriding. Nitrocarburizing is classified into two types i) Ferritic Nitrocarburizing and ii) Austenitic Nitrocarburizing, depending on the material phases and the transition. FNC is a low-temperature process in the ferrite region of the iron-carbon phase diagram. This process diffuses nitrogen and carbon into the surface of ferrous or non-ferrous materials at the temperature of 580°C. FNC process improves the surface characteristics like hardness, corrosion resistance, and wear resistance of low alloy steel. The surface is further enhanced by deliberately oxidizing the surface to produce a corrosion-resistant surface oxide barrier to the steel [24] [25].

Nitrogen and carbon are soluble in the steel surface at the temperature range 530°C– 600°C in the ferrite phase field. This process is usually performed in the salt bath furnace. The nitrogen penetrates from ammonia and diffuse into the steel surface along with carbon, and gets trapped with the interstitial lattice spaces in the steel structure. Nitrogen is more soluble than carbon and diffuses into the surface, while carbon forms the iron or carbide particles near the surface [25] [24] [26].

3.2.2. Transfer of Nitrogen and Carbon

The process is performed in the controlled atmospheric pressure and temperature range and the atmosphere's controlled composition. The atmosphere contains Nitrogen (N_2), Ammonia (NH_3), Carbon dioxide (CO_2), and Hydrogen (H2). Ammonia acts as a source for nitrogen, so in the Gas Ferritic Nitrocarburizing, ammonia will decompose into nitrogen and hydrogen, and the nitrogen will be soluble on the steel surface. This reaction is given in the equation below [24]

$$2NH_3 \rightarrow N_2 + 3H_2 \qquad \textit{Equation 1}$$

The part of ammonia that does not dissociate into nitrogen and hydrogen is called residual ammonia. This shows that the active nitrogen will diffuse into the steel surface and be saturated with the epsilon phase after nucleation. The carbon dioxide first diffuses into carbon monoxide, and carbon is produced by the reaction between the carbon monoxide and the hydrogen [24] [27].

$$CO + H_2 \rightarrow C + H_2 \qquad \textit{Equation 2}$$

The transfer rates of nitrogen and carbon into the steel surface entirely depend on their diffusion rate. The higher the concentration, the higher the transfer rate.

3.2.3. Compound layer

The Ferritic Nitrocarburizing process forms a nitrogen-rich compound layer at the steel surface and diffusion zone. This nitriding layer consists of two metallurgical phases, epsilon, and gamma prime nitrides [26]. Usually, the carburizing reaction is faster than the nitriding reaction, so the first step in forming the compound layer is the nucleation of cementite at the steel surface. The single-phase epsilon is ferritic nitrocarbide (Fe_3NC), a ternary compound that consists of iron, carbon, and nitrogen and has a crystal structure similar to the cementite structure [24]. The surface treatment continues the cementite structure is transformed into ε-phase, resulting in a homogenous epsilon layer formation. The next step is the formation of γ-phase ferritic nitride (Fe_4N) between the ε and surface. So this layer is formed by redistribution of nitrogen and carbon at the interface. The γ layer is the predominant layer compared to the ε layer. The γ-phase in the iron-carbon diagram is a stoichiometric compound with a narrow soluble range of

nitrogen and carbon [27]. This makes the γ layer grow slower, and the epsilon layer has a high soluble range and lets it grow quicker. The concentration phases control the growth of the compound layer. Decreasing the carbon content of the steel decreases the compound layer thickness [28] [29].

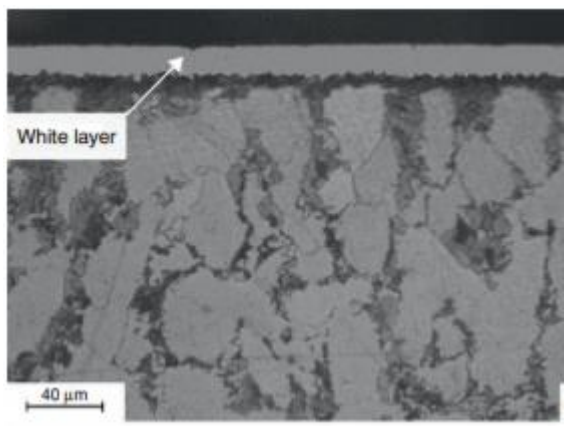

Figure 3: *FNC Compound layer [30]*

3.2.4. Porosity

The outer part of the compound layer, which is rich in nitrogen will contain pores. These pores are formed at the grains and boundaries and other discontinuities due to the longer processing time of nitriding and high nitrogen potential. The pores are formed when the interstitial nitrogen in the compound layer recombines to form nitrogen molecules. This step is also called as denitriding ($2N \rightarrow N_2$). Porosity in the layer can be controlled by adding the alloy element, which impacts the diffusion of nitrogen and carbon; as the alloy content increases, the diffusion decreases. Therefore, the pores are reduced [27].

3.2.5. Diffusion Zone

The diffusion zone is formed next to the compound layer, where nitrogen and carbon exist in the interstitial solid solution in the ferrite phase or alloy nitrides and carbides [23]. The diffusion zone is similar to the compound

layer, like an increase in the content of alloy nitrides and carbides increase the diffusion zone [25] [26] [27].

3.2.6. Properties

Nitrocarburizing a surface treatment process that improves the hardness wear resistance, fatigue, and corrosion resistance. The composition of the atmosphere and the alloy content processed at the temperature range 530°C-600°C to develop the properties [28].

3.2.7. Hardness

The main reason for the FNC treatment is to produce a compound layer that improves the hardness, wear resistance, and load-bearing capacity. The increase in the surface hardness increases the load-bearing capacity. The compound layer produces a uniform hardness throughout its cross-section area. The hardness of the FNC layer varies from 800-1000HV [27] [30]. The pores which are formed due to denitriding reduce the surface hardness. The hardness also depends on the alloy content of the steel grade. The concentration gradients of nitrogen and carbon determine the hardness of the diffusion zone. It shows how much nitrogen and carbon should dissolve on the surface and the processing temperature [24].

3.2.8. Wear Resistance

The compound layer determines the tribological behavior of the Ferritic Nitrocarburized surface. The wear resistance of the material is directly proportional to the surface hardness and is related to the steel's alloy content. So the nitrocarburized surface can produce less amount of wear if the abrading material is softer than the compound layer [24] [27].

Wear resistance is influenced by hardness; the ceramic nature of the compound layer will lower the friction with the abrading material and prevent the surface from welding together, so the resistance is increased. The presence of ε-phase nitrides increases the wear resistance of the layer. But when the compound layer wears off, the resistance towards abrasion will

drastically reduce, so the increase in the depth of the compound layer will increase the wear resistance [24] [27].

3.2.9. Corrosion Resistance

One of the main advantages of performing the nitrocarburized treatment is increasing the corrosion resistance of the steel. These nitrocarbides in the noble phases form a dense layer underlying the steel surface to protect from corrosion [24]. The ε-phase has better corrosion properties than the γ-phase due to the crystal structure, and the nitrogen content is higher in the ε-phase. The quantity of the epsilon phase in the compound layer plays a vital role in corrosion resistance. And the poor pores will decrease the corrosion effect [31].

3.2.10. Post-oxidation of FNC treated GCI (Corr-I-Durr)

Post-oxidation is another vital process in nitrocarburizing in improving corrosion resistance. The oxidation process is performed over the treated surface at the temperature range 450°C to form another protective Fe_3O_4 layer. This layer thickness varies from 1µm to 2µm. Post oxidation will reduce the formation of pores over the compound layer, which increases the corrosion resistance. The oxide film formed will protect the metal surface in contact with the air and reduces oxidation. The oxidized layer is in attractive black color [24].

3.3. Brake pads

Brake pads are components of brake discs. The disc brakes are used to slow down or stop the vehicles by pushing brake pads against the brake discs. The friction and wear process between the brake pad and the brake disk determines disc brake quality [32]. The brake pads are generally divided according to different contents of ingredients into three types Low Metallic (LM), Semi-Metallic (SM), and Non-Asbestos Organic (NAO) brake pads [33]. Automotive Components Floby AB supplied the Non-Asbestos Organic (NAO) brake pads for the thesis work. A polymer/ceramic/metallic fiber, binder, filler, abrasive, and solid lubricant make up typical NAO pads. The lining gains strength, stiffness, thermal stability, wear resistance, and

stable frictional properties due to the fibrous reinforcement [34]. The NAO brake pads have low noise when braking, and the wear rate is low, but the disadvantage is they lose their braking capacity at high temperatures [32]. These NAO brake pads are used in countries like the USA, India, and other Asian Countries.

3.4. Tribology

The Word' tribos' means rubbing or sliding in Greek. In tribology, the basic that we investigate is the friction, wear, and lubrication under a controlled condition [35].

3.4.1. Friction

When the Two interacting surfaces are in relative motion, the resisting force to the relative motion is called the Friction [35]. The COF is affected by temperature, material property, surface roughness, and hardness [35]. The two kinds of friction that we observed are static friction and dynamic friction. The ratio of maximum friction force prior to the normal force acting on the load at rest is called static friction. Dynamic friction is the ratio of friction force to the normal force acting on the load during sliding.

The Amontons- Coulomb laws of friction [36]
The friction force is proportional to the weight of the body moved.
The frictional force is independent of the contact area.
The frictional resistance is independent of sliding velocity.

$$F_t = \mu * F_n \qquad \textit{Equation 3}$$

Where F_t is tangential force, μ is Coefficient Of Friction (COF), and F_n is the normal force

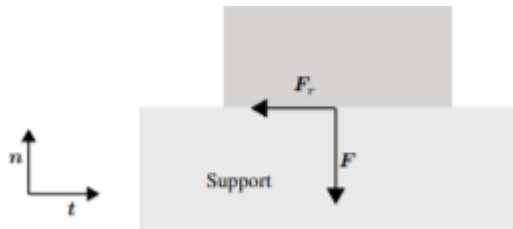

Figure 4: *Schematic of a body sliding on a flat surface of a rigid support [37]*

When discussing the friction coefficients, there are two types of contacts dry and wet contacts. Where wet contacts we use lubricants, with good lubricants, the coefficient of friction will below. The brake disc and brake pads have a dry contact. For dry sliding contact, the friction coefficient for most common materials will range from 0.2-0.6 [38]. The friction coefficient may vary, which is shown in the below Figure 5.

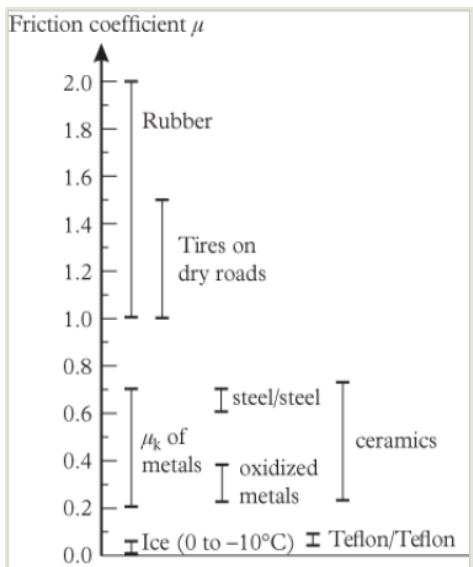

Figure 5: *Range of friction coefficient values for some materials under dry sliding conditions [38]*

3.4.2. Wear

Wear is characterized as damage to a solid surface caused by relative motion between that surface and a contacting substance, which usually involves progressive material loss [39]. The wear plays a significant role in the COF for a given system. Wear results in the formation of the tribological interface in the brake discs. Types of wear are i) Adhesive wear, ii) Abrasive wear, iii) Fatigue wear, iv) Chemical wear. Wear development is dependent on sliding velocity and the force components.

3.4.3. Tribological Interface

In the tribology of the brake discs, wear plays a vital role. Due to the wear, the particles are removed from the surface of brake discs and pads, which are crushed and milled down to tiny particles. These wear are trapped between the contact interface of brake surfaces [40] [41]. These mixed particles when it gets oxidized they form a third body or film. The third body will consist of all the elements from brake discs and the friction linings, including their oxides [42]. The interface composition depends on the loading conditions. The presence of the third body will increase the COF. If the third body is blown off from the pads, the COF will reduce. The third body will reduce the wear by preventing direct contact with the discs and pads [43].

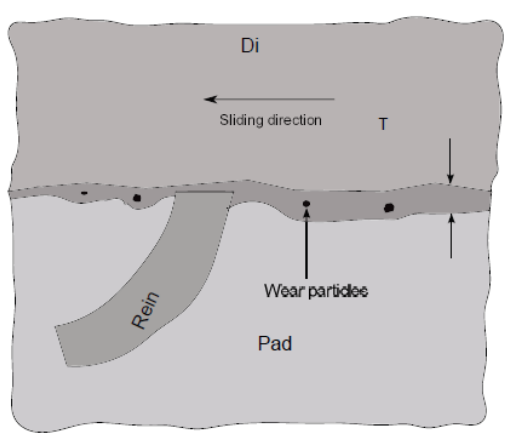

Figure 6: *Schematic representation of interface between brake discs and pads [42]*

3.4.4. Tribology Behaviour

3.4.4.1. Coefficient Of Friction (COF)

Since drivers assume the same degree of friction force at all braking conditions, the change in a brake's COF as a function of sliding speed and applied pressure is a critical problem [44]. Noise, anti-fade, and vibration are all related to changes in the COF.

The tribological parameters like friction and wear of the brake discs depend on the contact conditions, which depend on the design of the brake disc system. The contact conditions are sliding velocity, braking pressure, contact area, temperature, humidity, surface geometry, etc. These contact conditions are not constant and vary in time and space during braking. The pressure and COF are indirectly proportional to each other; when the pressure increases, the COF decreases [45]. When the braking pressure increase, the contact area surface will increase, and once they reach a stable value, the COF start to decrease [46]. Increase in the contact area for the engaged plateaus, and also more contact plateaus become engaged. Furthermore, the increase of actual contact area with the formation and growth of the secondary contact plateaus reduces the COF [47] [48]. When the sliding velocity is low, the friction between the brake pads and discs will be low, and COF also lows [49] [50]. So the increase in sliding velocity will increase the surface temperature between the sliding pairs, which leads to the formation of the tribofilm. The tribofilm formed is consists of oxide layers. When the tribofilm gets thicker, it starts to shear, and COF will increase [51] [48].

The friction coefficient is affected by the microstructure of the material. The amount of graphite flakes strongly affect the damping capacity and thermal conductivity of iron. The higher the content of graphite increases the COF [52]. The hard particles like SiC present in the GCI will not plastically deform at the contact surface because of their angular structure. The SiC scratches the counter surface material, which is oxidized at a high temperature. SiC particles have high friction coefficient due to their inherent hardness property [53].

3.4.4.2. Wear Rate

The material transfer will occur during the severe wear regime and is welded to the brake pads. The GCI discs usually show a low wear rate due to the presence of ferrite [54] [55]. GCI exhibits excellent wear resistance to graphite film formation during dry sliding wear conditions. Graphite in GCI acts as a solid lubricant forming the tribofilm and reduces both friction and wear of the brake discs.

The wear rate and the sliding velocity are directly proportional. When the sliding velocity increases, the wear rate also increases [56]. At the initial braking condition, the wear rate will be high because of the plastic deformation, cutting, and dropping of asperities on the contact surface. The mechanical actions with the asperities become increasing with a rise in velocity [56]. The braking pressure also affects the wear rate. When the pressure increases, the wear rate also increases. The braking pressure has an effect on the cutting depth of asperities.

3.5. Chapter summary

The chapter starts with Gray Cast Iron brake discs and different layers in the brake discs. Later, it discusses the coatings like oxides, carbides, and alternative materials used so far in the brake discs. The next part is about the disadvantage of coatings and the need for the surface treatment process. The second section of the chapter explained the Ferritic Treatment process in detail, working methods, and the properties of nitrocarburized steels. The third section of the chapters discuss the brake pads. The later section of the chapter explains the tribological behavior and how it varies.

4. Experimental Methodology

This chapter explains the machines used for the experiment and the procedure the authors followed during the project work.

Automotive Components Floby AB supplied three different brake discs for the project i) Gray Cast iron, ii) Ferritic Nitrocarburized Gray Cast Iron, and iii)Oxidised Gray Cast iron (Corr-I-Durr). The brake disc 345 mm in diameter. The brake discs are cut into the required dimensions using the band saw machine. The brake disc is cut to a length of 200 mm and width 30 mm and the brake pads are cut to a 20*20 mm^2 with 45° chamfer on all four sides. A small piece is cut from the leftover brake disc where the cross-section should contain the coated layer for the sample preparation.

Figure 7: *Band saw machine*

a) Before

b) After

Figure 8: *Before and after cutting of brake disc*

Figure 8 shows the brake disc before and after cutting using the band saw machine. The large rectangular bars are used for the tribotesting experiment, and the small pieces are used for sample preparation and microstructure analysis.

4.1. Tribotester

Tool information- The authors used the brake pads as the tool, and it is cut to a dimension of 20*20 mm^2 with chamfer as shown in the below figure.

Figure 9: *Tool*

The procedure that was carried out when performing the tribotester

1. The test matrix is created for different pressures and velocities.
2. The workpiece material is cleaned and placed in the workpiece holder.
3. Then the brake pad is placed in the tool holder.
4. During the test, the tool slides over the workpiece material in a linear motion with pressure and velocity.
5. The test is performed for 100 passes for one workpiece with the same condition. All six conditions in the test matrix were completed for one workpiece material on each new side.
6. After every three conditions are performed, a new tool is used.
7. The workpiece material is changed, and the same procedure is repeated.

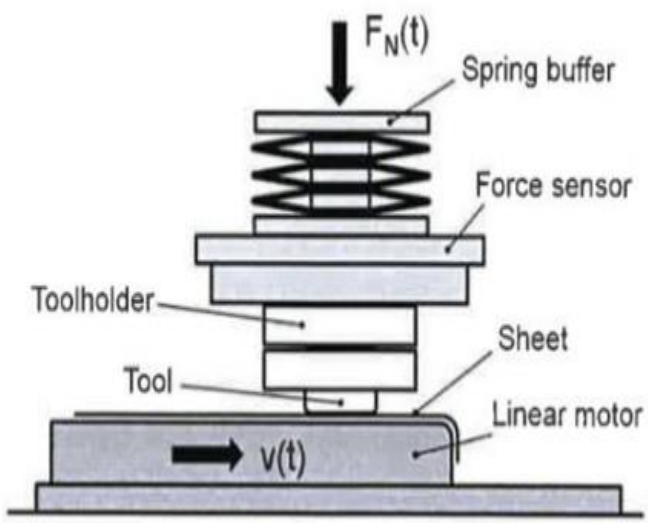

Figure 10: *Schematic illustration of the test setup of the tribotester [57]*

Test matrix

The chosen experimental conditions are provided in Table 1. These conditions were selected based on the limitation of the tribotester machine used. The values used for the tribotesting experiment are pressures 0.75 MPa, 1.5 MPa, and 2.5 MPa and two sliding velocities of 0.1 m/s and 0.3 m/s. These pressure values are considered smooth braking, medium braking, and sudden braking as these values do not represent the same as real-life situations. The experiment is performed for 100 passes for each condition for all three brake discs.

4.2. Sample Preparation

4.2.1. Mounting data

The CitroPress-5/-15/-30 machine was used for mounting the workpiece.
The heating and the cooling times in Table 2 referred to the following conditions.

- The total process time counted from the start of the process and not from when the pre-set temperature is reached for the heating time referred to in Table 2.
- The mounting parameters are calculated using specimens that makeup around 20% of the total volume of the mount.
- When mounting smaller specimens or specimens with low heat conductivity, the heating and cooling times should be increased. To avoid porous in the cured mount, it may be important to increase the pressure.
- To avoid the cotton ball effect, higher pressure is recommended with ClaroFast.
- The amount of resin is added to reach the final height of the sample mount of approximately 20 mm.
- If several reasons are combined in one mount, use the process parameters for a cause with the most extended times. When using CitroFast as backing, use the CltroFast process parameters. For very complicated specimens, add one minute of heating time.

On all CitoPress models, three pre-set cooling levels are available high, medium, and low.

For optical and SEM samples, polyfast resins were used to prepare them. The following data mentioned in Table 2 is used for mounting the samples.

Table 2: *Mounting Data*

Cylinder	Resins		Heating			Cooling		Time
25 mm	Type	Quantity	Time	Temperature	Pressure	Time	Rate	Total time
		ml	min	°C	Bar	min		min
	PolyFast	15	3.5	180	325	1.5	High	5

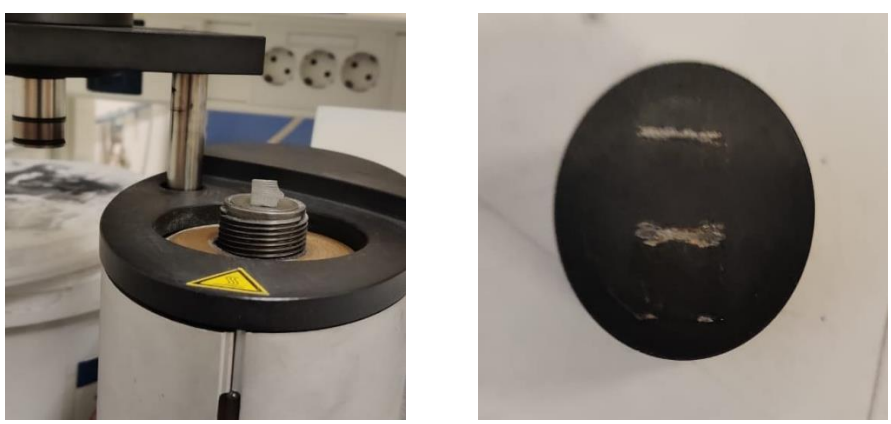

a) Before *b) After*

Figure 11: *Before and After mounting*

In Figure 11, the workpiece was kept in a sectional view where the coated layer should be visible, and the process is conducted as mentioned in Table 2.

The mounted samples were polished using the Tegramin-30 machine.

The polishing of the workpiece is peformed in 5 steps with a pressure of 10N and of RPM 150 and each step.

1. In the first step, the SiC foil 220 pads were used with water as a lubricant on the mat to remove the epoxy and make a flat surface of the workpiece.
2. The second step is using the Md-plan – DiaPro All/lar mat, and it removes 9µm is removed from the surface, and the workpiece is smoothened.
3. In the third step, the MD-Dac – DiaDuo-2 3µm mat was used, which removes 3µm is removed from the workpiece and smoothens the workpiece more.
4. MD-Dap – DiaDuo-2 1µm mat was used in the fourth step to remove 1µm fine particles and smoothen the surface of the workpiece.
5. The authors used MD-Chem OP-U NonDry for further smoothening the workpiece.

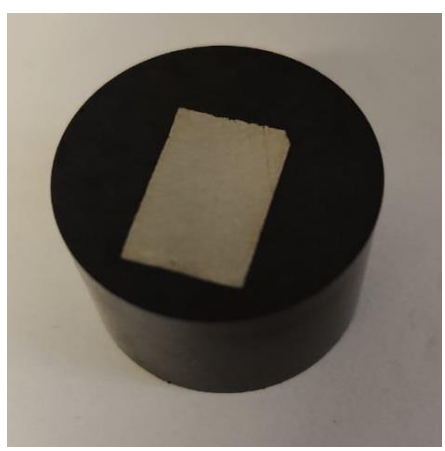

Figure 12: *Workpiece after polishing*

4.2.2. Etching

After the polishing, etching for the samples is performed. Etching is done to enhance the contrast on surfaces to get a better microstructural characteristic of the sample, which is not evident in the polished condition.

In etching, 1-5 ml of HNO_3 and 100ml of ethanol (95%) were used. When the etching rate increases, sensitivity decreased with the increased percentage of HNO_3.
The process for etching the sample

1. The sample was immersed in 5% of HNO_3 solution for 5-40 seconds. And then, the sample is immersed for 25 seconds in 10% of HCL-methanol solution to remove the stain.
2. The sample was then swabbed or immersed for 30 seconds.
3. After immersing the sample, it was transferred to a water bath, and again then the sample was kept in the ethanol vibration bath for 15 minutes, and compressed air was used to dry the sample.

4.3. Microscope

The optical microscope system gives the accurate 3D measurement of surface roughness, vertical resolutions up to 10 nanometres. The principle of this system is focus variation technology. Focus variation uses a technology that combines the focus from the small depth of an optical system with vertical scanning to provide the surface characteristics from the varying focus [58]. The light source is focused on the specimen. The light is then reflected in several directions as soon as it hits the specimen via the objective. The rays from the specimen and hitting the objective lens are bundled in the optics and gathered by a light-sensitive sensor behind the splitting mirror [58]. Now small regions of the object are sharply imaged. Then move the lens vertically down the optical axis for the detailed view. Now the acquired data is converted into 3d data by the sensors, and the sharp images of the surface are produced.

4.3.1. Scanning Electron Microscope (SEM)

A scanning electron microscope (SEM) produces a magnified image of the sample by scanning it with an electron beam over the sample's surface and providing information about the sample's surface topography and composition [59] [60].

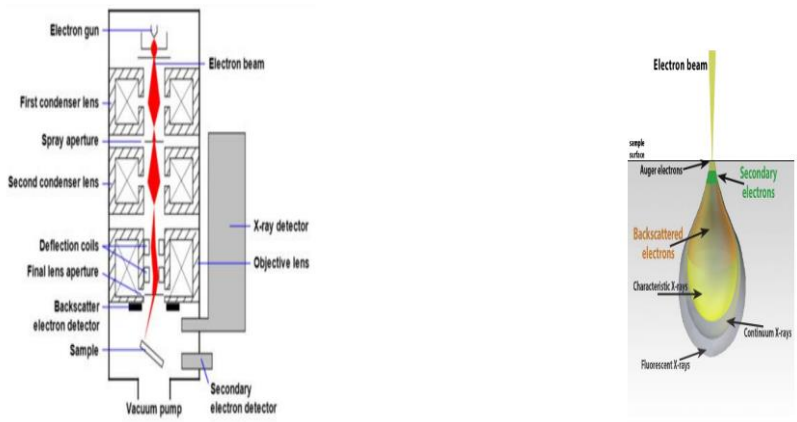

Figure 13: *Schematic of SEM interaction [59]*

The major component of the scanning electron microscope is the electron gun that creates a beam of electrons. The amount of electrons that move down the column is regulated by the condenser lens. The beam is focused onto a spot on the sample by the objective lens, deflection coil, which helps deflect the electron beam, and secondary electron deflectors (SED) attracts the secondary electrons. Additional sensors detect backscattered electrons and x rays [59]. The electron gun acts as a source for electrons placed at the top column. These electrons move downwards by passing through series of lenses called the condenser lens. There are two condenser lenses, namely primary and secondary condenser lenses. The electrons are assembled and are made a fine beam by the condenser lens. And the objective apertures produce a focused beam of electrons that hits the surface of the sample. The signal is sent to a computer monitor. The vacuum level will be determined by the microscope's configuration [61]. Coils situated above the objective lens control the electron beam position, which helps scan the sample's surface. This beam scanning the surface collects information about a defined area on the sample. As a result of the electron-sample interaction, several signals are produced, and appropriate detectors then detect these signals [59]. The scanning electron microscope never forms an actual image of the sample; instead, a virtual image is constructed from the signals emitted by the sample.

As the electron beam interacts with the sample and penetrates the sample to a depth of a few micron signals like secondary electrons, backscattered

electrons, and characteristic X-rays are produced. An image of the sample can be obtained and displayed by measuring the flux of one of these types of particles as a function of raster or scan position. Backscatter electron is the electrons that are deflected back in the direction of the beam. The detector traps signal and is used to determine the areas and the atomic number of the elements present in the sample. If the atomic number is low, the backscattered electrons will be less and appear less bright, and if the atomic number is more, there will be more backscatter electrons, and it will be brighter in color [60]. The secondary electrons are collected, giving information about the sample the topographical features [60]. Element and mineral information can be found out from the x-rays. Scanning electron microscope SEM produces black and white images and three-dimensional images.

Figure 14: *Tescan Machine*

Experiment procedure

The sample selected for the SEM analysis is a coin-shaped structure. Before observing the sample through the microscope, it should be prepared. The sample had been cut, and it is polished using fine sandpaper. The sample is then washed with the cleaning agent containing silicon oxide. Finally, the sample was cleaned using Ultrasound Vibrations before being inserted into the SEM chamber.

First, the sample is observed through the optical microscope. The optical microscope is used to identify the surface structure of the sample. Then the material is placed in the vacuum chamber of the SEM. The SEM provides detailed information about the topographical and chemical composition. The SEM has two electrons, Secondary Electrons and Back Scattered Electrons, that provide different microstructure images of the sample. The brightness and contrast have been adjusted for a better quality of the images. Therefore several spots were identified.

4.4. Hardness

The brake disc's hardness is measured using the Vickers hardness machine. Hardness is a ratio of loading force to an actual contact area.

$$HV = \frac{1.8544 * F}{d^2} \qquad \textit{Equation 4}$$

Where F is the loading force and d is the diameter.

The Vickers hardness machine has a diamond intender tip. When the sample is placed, and the machine is started, the sample's diamond intended shape is formed. A microscope is used to measure the two diagonals of the indentation left on the material's surface after the load is removed. The average is determined, which is used for calculating the hardness. The load force is 2kg and dwells time 10 seconds the values taken for experimenting.

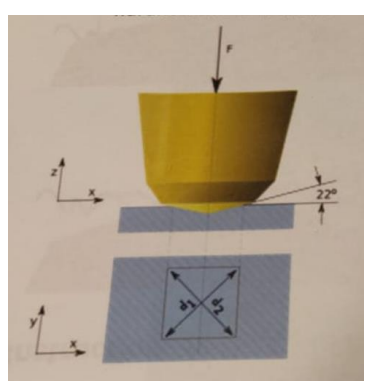

Figure 15: *Schematic of Vickers hardness measurement*

4.5. Chapter Summary

The chapter discusses the equipment used for the experiment's setup. The first part discusses the tribotesting and test matrix performed to analyze the wear and coefficient friction of the brake discs. The next part explains the etching process to improve the contrast for better microstructure analysis. The later section explains the procedure to analyze the microstructure. The final part of the chapter explains the Vickers hardness procedure.

5. Results

This chapter discusses the experimental results that were obtained in the study.

5.1. Microstructure

The microstructure of the samples was analyzed using SEM and Aliciona microscope after an etching technique. The etching technique helps to identify the different phases in the structure and the solidification structure.

5.1.1. Gray Cast Iron

Figure 16 presents the microstructure of the GCI brake disc. This microstructure is in the pearlitic matrix formed by the eutectoid reaction. This pearlite matrix comprises both ferrite and cementite phases. The thick white layers are the ferrite phase, and the thin lamellae are the cementite phase which appears dark. The graphites flakes are in an average length of 45µm. Graphite present in the GCI will conduct heat from the sliding interface. The main constituents of this GCI are Carbon, Iron, and Oxygen. The other constituents include Silicon, Sulphur, Manganese, Chromium, Aluminum, Phosphorous. The sulphur content in the GCI promotes the high hardness in the pearlite matrix. The yellow spots indicate the sulphur in the microstructure. And the different colors indicate the other constituents in the present GCI microstructure.

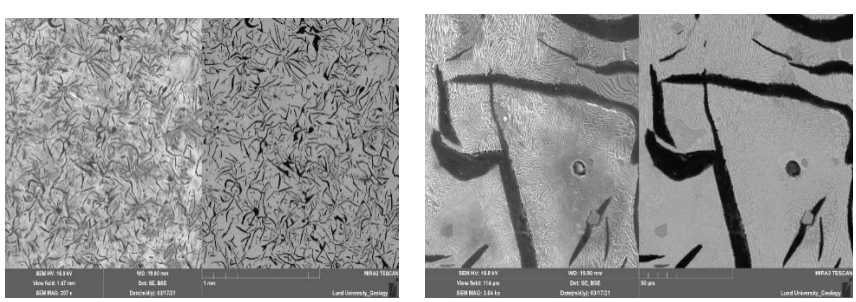

a) 1mm *b) 50µm*

Figure 16: *SEM view of GCI Microstructures a) 1mm and b) 50µm*

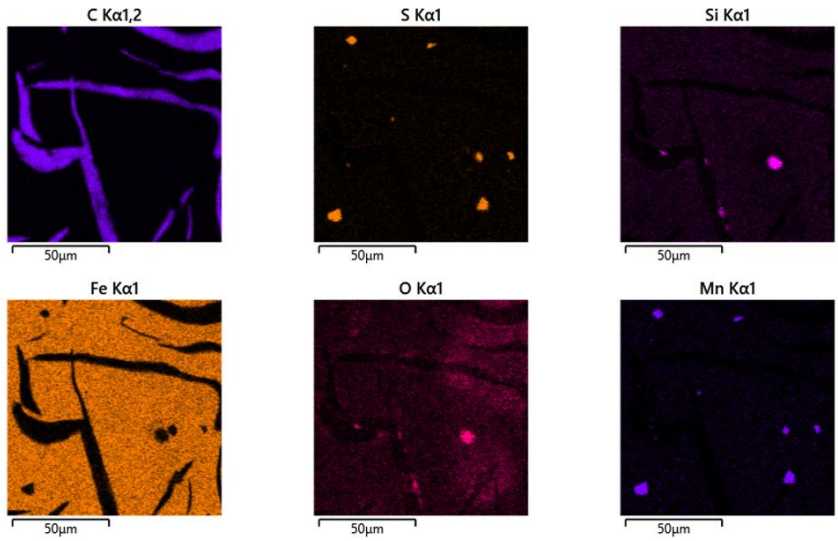

Figure 17: *Elemental SEM-EDS mapping of GCI microstructure.*

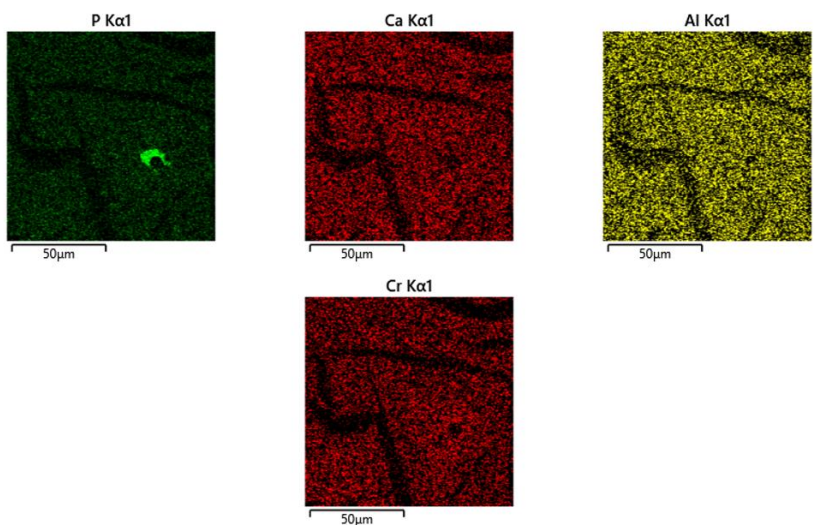

Figure 18: *Elemental SEM-EDS mapping of GCI microstructure.*

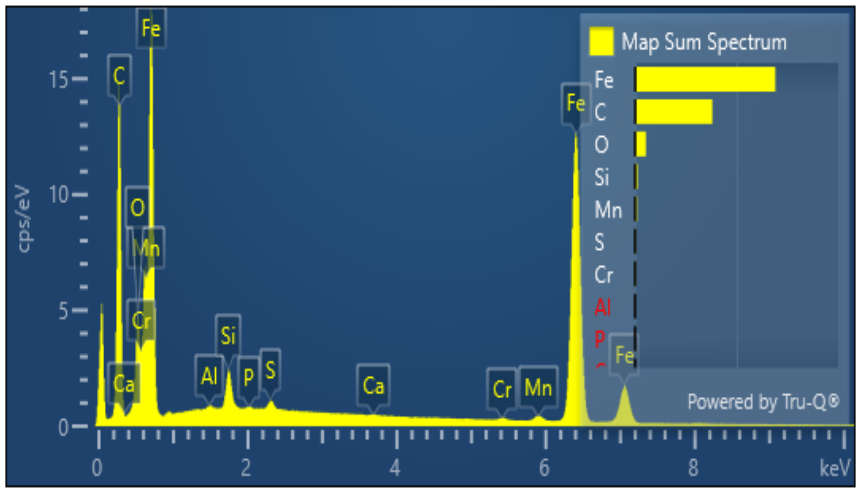

Figure 19: *EDX spectra of GCI brake disc*

5.1.2. Ferritic Nitrocarburizing (FNC)

The FNC samples microstructure was investigated using the SEM at the magnification of 50µm.

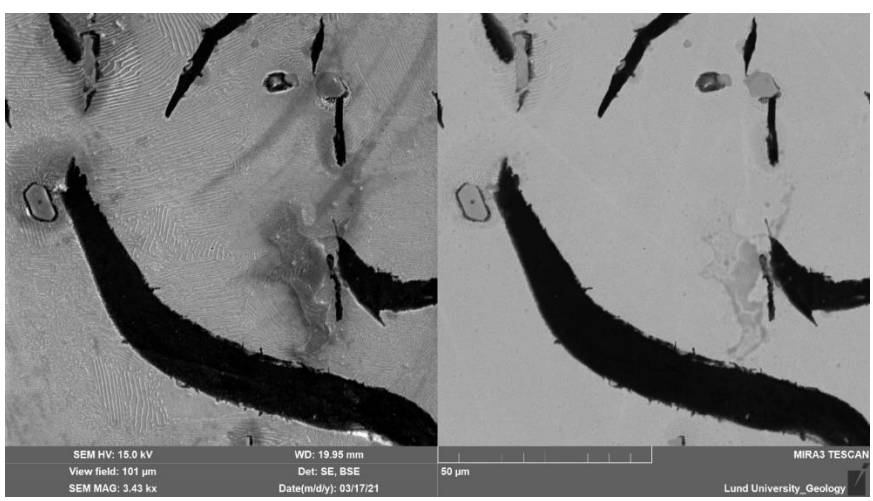

Figure 20: *SEM analysis of FNC microstructure*

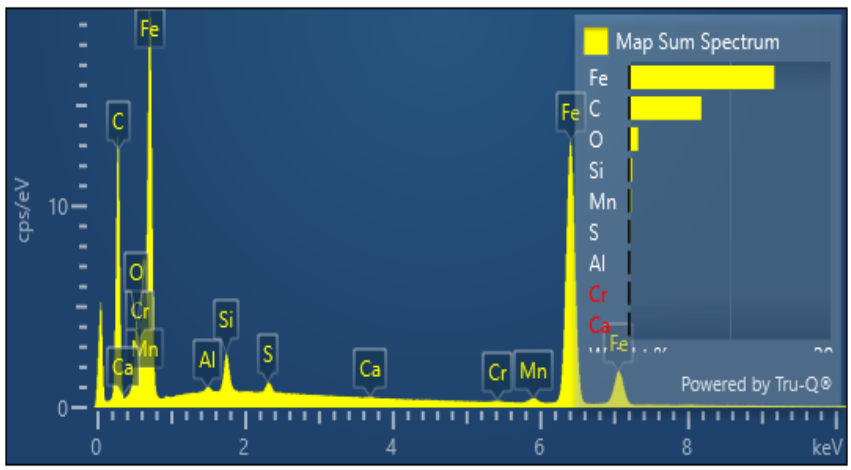

Figure 21: *EDX spectra of FNC brake disc*

The FNC samples have the same microstructure similar to the GCI samples. FNC samples have the compound layer which is formed by the diffusion of carbon and nitrogen into the surface. The compound layer thickness of the nitrocarburized samples was examined in etched conditions. The post-oxidized FNC (Corr-I-Durr) will have an oxidized layer. But the additional oxidized layer is not found in the Corr-I-Durr sample. These FNC samples have the compound layer of range 10µm to 50µm. The compound layer thickness is not uniform throughout the sample, as shown with arrows in Figure 22. The uniform thickness may be due to the increase in the carbon content of the substrate.

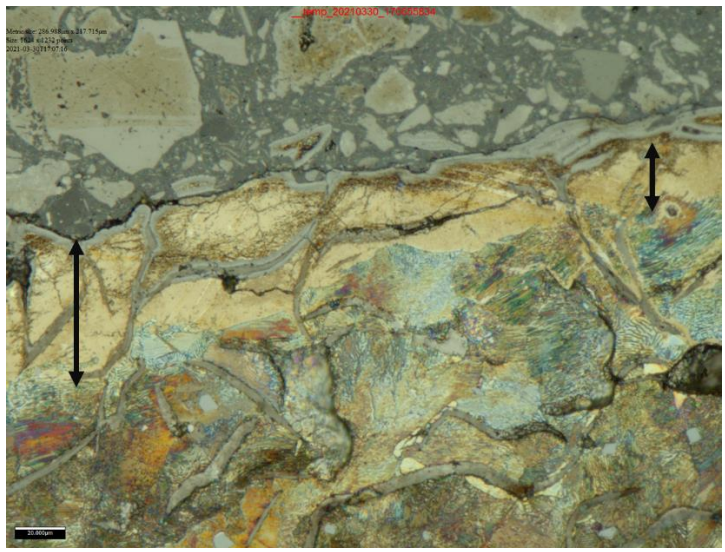

Figure 22: *Compound layer of FNC samples with thickness 48µm*

5.2. Surface Hardness

The hardness distribution in a material affects its properties, such as load-bearing capacity and fatigue resistance. A depth-sensing Vickers micro indenter was employed to measure the Vickers microhardness. The load of 2 kg and a dwell time of 10 seconds were used for the FNC treated and untreated GCI. The reason for selecting 2 kg is that some of the FNC samples have the softcore. The Vickers microhardness was calculated on all the brake discs by measuring the indentation diagonals. A minimum of 8 indentations was performed for each hardness measurement. Figure 23 shows the values of Vickers Hardness measurement.

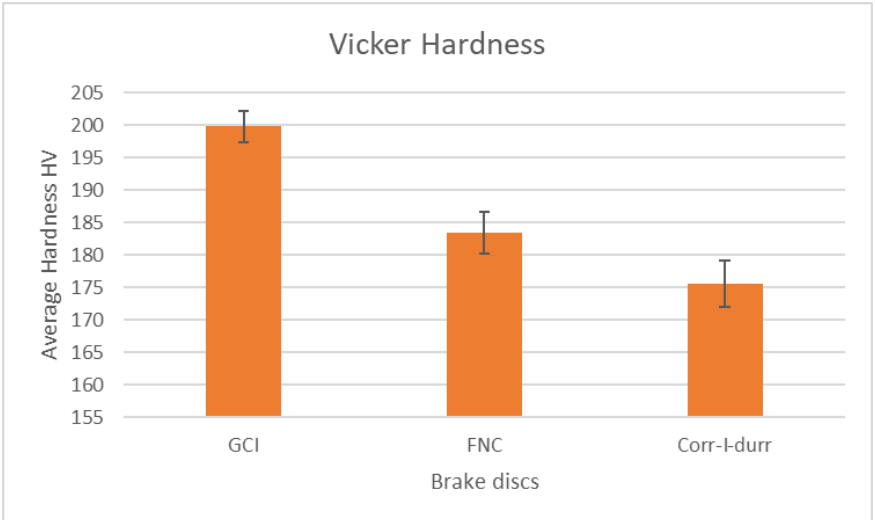

Figure 23: *Surface hardness of FNC treated and untreated brake discs*

Figure 23 shows that the untreated GCI brake discs have high higher hardness when compared to the FNC and Corr-I-Durr brake discs. The compound layer of the Ferritic nitrocarburized samples is not homogenous through the surface, and the hardness of the FNC depends on the depth of the compound layer. Corr-I-Durr shows comparatively lower hardness to FNC-treated GCI and the untreated GCI. The composition of the base material also determines the hardness of the surface. If the carbon content is low, it forms the softcore over the surface, resulting in the lower hardness for the FNC brake discs.
In the nitrocarburized samples, the micro indentor breaks the compound layer and reaches the surface, resulting in lower hardness compared to untreated GCI.

5.3. Coefficient of Friction (COF)

The tribology experiment was performed on the different brake discs to determine their performance relating to the COF and wear. The experiment was conducted for the different test conditions. The experiment was carried out for 100 passes for the same workpiece for the same test condition.
The following Figure 24-Figure 26 shows the COF for different brake discs and different test-conditions.

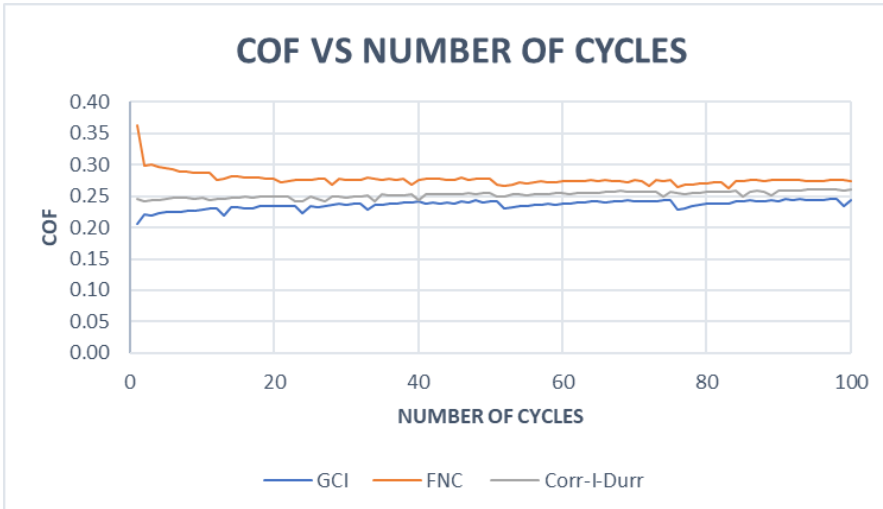

Figure 24: *Coefficient of friction vs number of pass for velocity 0.1m/s and 1.5MPa*

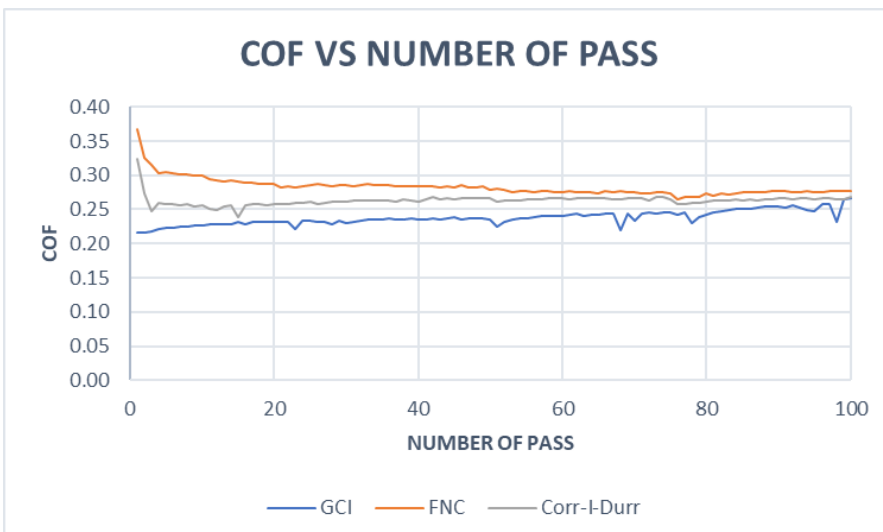

Figure 25: *Coefficient of friction vs number of pass for velocity 0.3m/s and 1.5MPa*

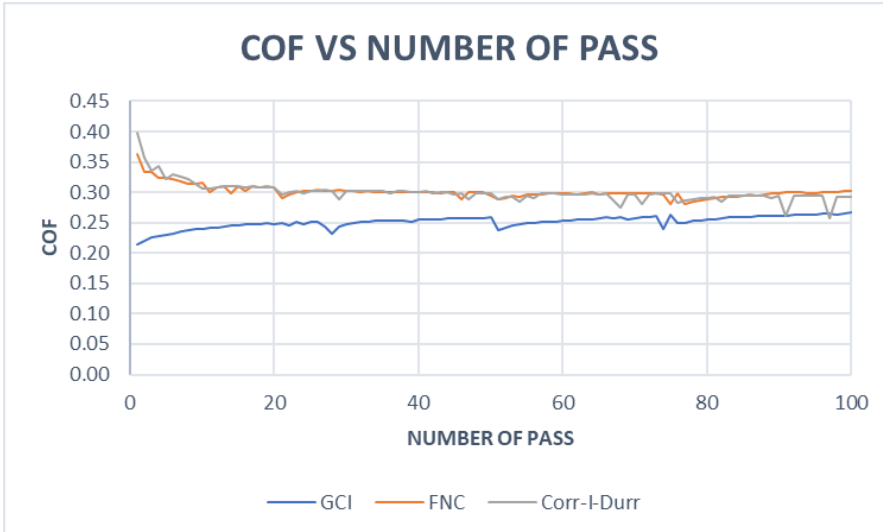

Figure 26: *Coefficient of friction vs. number of pass for velocity 0.3m/s and 2.5MPa*

Table 3: *The table showing the different test conditions and their mean coefficient of friction values for different brake discs GCI, FNC, and Corr-I-Durr*

Velocity(V) m/s	Pressure (P) MPa	Mean COF of GCI	Mean COF of FNC	Mean COF of Corr-I-Durr
0.1	0.75	0.22207	0.28752	0.25627
	1.5	0.23881	0.27434	0.25379
	2.5	0.2501	0.28185	0.26639
0.3	0.75	0.21615	0.24371	0.27864
	1.5	0.24056	0.2784	0.26391
	2.5	0.25461	0.29741	0.29475

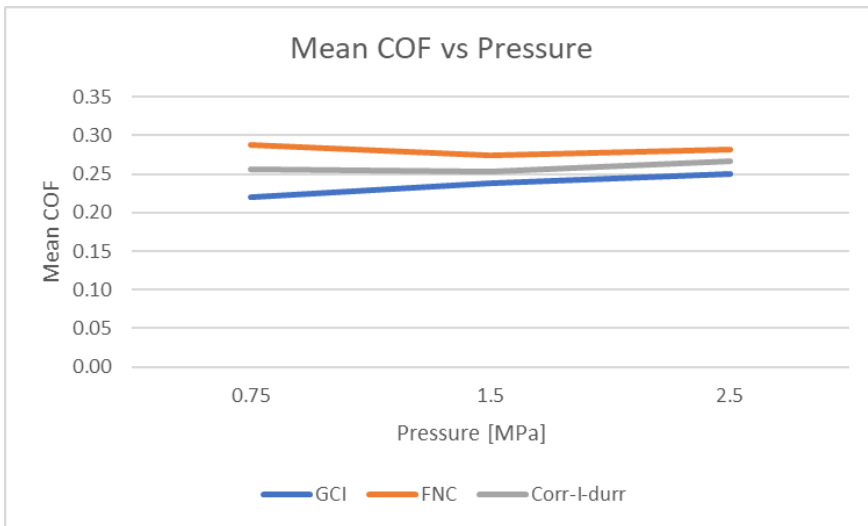

***Figure 27**: Mean Coefficient of friction vs different brake discs with varying pressure for velocity 0.1m/s.*

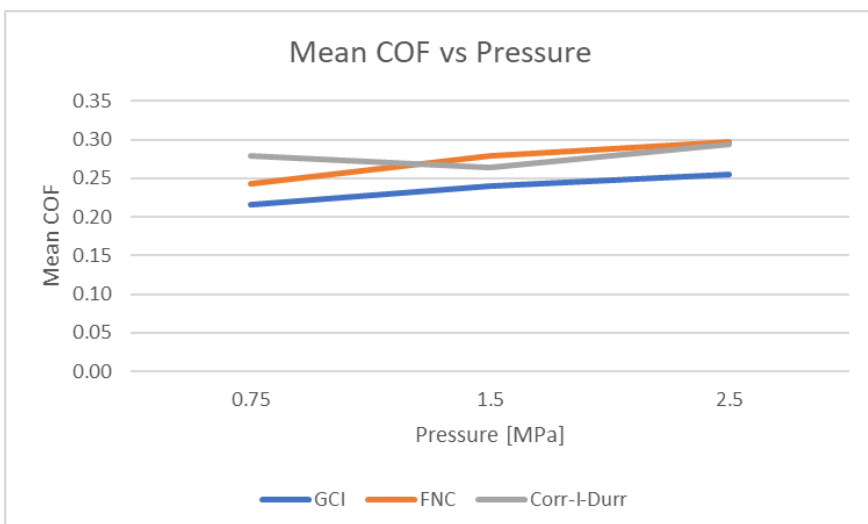

***Figure 28:** Mean Coefficient of friction vs different brake discs with varying pressure for velocity 0.3m/s.*

During the typical test, the COF tends to rise initially, and then it settles to the steady-state level after 10-15 slides in the range between 0.26-0.3 for

FNC treated brake disc. This general trend was common for the FNC-treated brake discs regardless of the compound layer and the oxidized layer depth. But this is different in the case of untreated GCI. The coefficient of friction starts to increase and reach a stable value between 0.22-0.25. The average values starting from passes 20 to 100 were considered in calculating the mean coefficient of friction. Table 3 describes the mean coefficient for different brake discs.

Figure 27 and Figure 28 show a variation in COF with pressure with varying velocity 0.1 m/s and 0.3 m/s. At the low-velocity 0.1 m/s, FNC shows higher cof compared to GCI and Corr-I-Durr brake discs. The FNC treated brake discs vary when the pressure increases; it shows high COF for 0.75 MPa and gradually decreases for the pressure 1.5MPa. And again, it increases for the pressure of 2.5MPa. This may be because of the tribofilm formation. But in the case of GCI brake discs, the COF rises with increasing pressure.

At velocity 0.3 m/s, the COF increases for both GCI and FNC brake discs when the pressure rises. From the above results, it can be observed that both the velocity and pressure affect the COF of brake discs.

Figure 27 and Figure 28 clearly shows that at a certain velocity and increasing pressure, the COF increase. The mean COF of different brake discs is GCI - 0.22, FNC - 0.27, and Corr-I-Dorr - 0.26. So the FNC treated brake discs show higher COF compared to other different brake discs used.

5.4. Wear

The tribology experiments were performed to determine the wear and COF. The brake pads slide against the brake disc when the load acts on it. The weight loss of the pads before and after every 25 slides was measured using an electronic weighing machine with the accuracy of 0.0001 g to measure the wear rate of the pads. The brake pads were cut to the dimension of 20*20 mm. Two tools are used for the same workpiece material. First Tool is used for the condition 0.1 m/s velocity and different pressures 0.75 MPa, 1.5 MPa, and 2.5 MPa. The second Tool is used for the velocity 0.3m/s and different pressure 0.75MPa, 1.5MPa, and 2.5MPa conditions. The same kind of tool setup is used for other workpiece material, and the change in the weight of the tools is shown in the table below.

Table 4: *Change in pad weight (Tool) after different sliding passes for GCI brake discs*

Tool	0	25	50	75	100
1	32.3621	32.3621	32.3616	32.3616	32.361
1	32.3610	32.3603	32.3584	32.3574	32.3562
1	32.3562	32.3542	32.353	32.3514	32.3510
2	28.1965	28.1965	28.1960	28.1958	28.1955
2	28.1955	28.1949	28.1944	28.1940	28.1928
2	28.1928	28.1914	28.1899	28.1888	28.1876

Table 5: *Change in pad weight (Tool) after different sliding passes for FNC brake discs*

Tool	0	25	50	75	100
3	28.3606	28.3241	28.3105	28.3048	28.3018
3	28.3018	28.2841	28.2773	28.2724	28.2708
3	28.2708	28.1998	28.1847	28.1737	28.1660
4	31.6463	31.6125	31.6052	31.6012	31.5986
4	31.5986	31.5807	31.5734	31.5670	31.5623
4	31.5623	31.5200	31.5023	31.4898	31.4818

Table 6: *Change in pad weight (Tool) after different sliding passes for Corr-I-Durr brake discs*

Tool	0	25	50	75	100
5	32.0339	31.9715	31.9634	31.9578	31.9540
5	31.9540	31.9450	31.9398	31.9360	31.9317
5	31.9317	31.8835	31.8747	31.8700	31.8641
6	31.3546	31.2667	31.2595	31.2536	31.2510
6	31.2510	31.2050	31.2060	31.2011	31.1975
6	31.1975	31.1528	31.1362	31.1247	31.1157

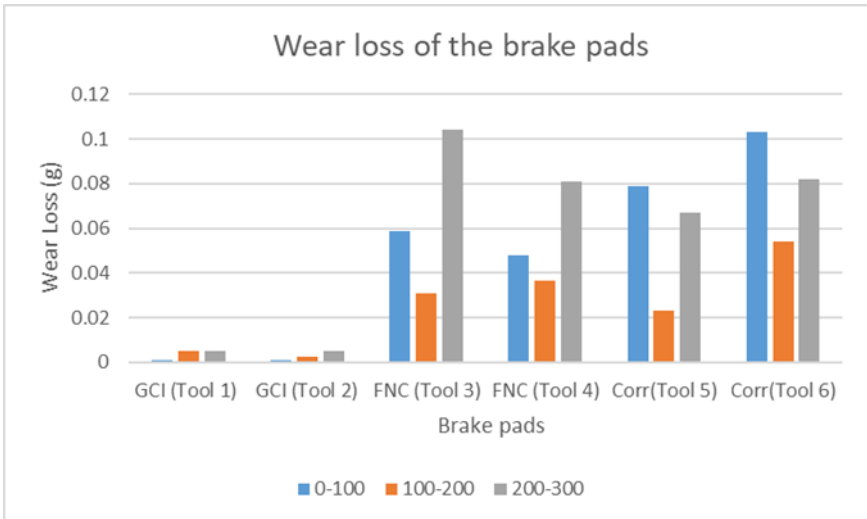

Figure 29: *Pad wear loss against various GCI brake discs and at different sliding passes*

The specific wear rate of the brake pads were calculated using the formula [48]

$$k = \frac{\Delta m}{\rho * F_N * S} \qquad \textit{Equation 5}$$

Where Δm represents the mass loss of the pads, ρ is the density of the brake pads, F_N represents the normal force acts between the pads and the discs, S is the sliding distance during the test. The density of the braking friction material is 2.75g/cm^3.

Figure 29 show that the tool used for FNC-treated brake discs significantly shows a high wear loss compared to untreated GCI brake discs. Initially, in FNC-treated brake discs, wear loss is high for the first 100 passes (for the pressure 0.75 MPa), then it gradually decreases for the next 100 passes (for pressure 1.5 MPa). For the pressure of 2.5 MPa, the FNC brake discs show high wear. So it is clear that pads used for the FNC brake discs will be worn out more compared to the tools used for GCI brake discs.

Table 7: *Table showing the wear coefficient of FNC treated and Untreated GCI brake discs for different sliding conditions.*

Velocity(V) m/s	Pressure (P) MPa	Wear coefficient of GCI m^3/Nm	Wear coefficient of FNC m^3/Nm	Wear coefficient of Corr-I-Durr m^3/Nm
0.1	0.75	$7.1301*10^{-12}$	$4.192*10^{-10}$	$5.696*10^{-10}$
	1.5	$1.7*10^{-11}$	$1.105*10^{-10}$	$7.95*10^{-11}$
	2.5	$1.112*10^{-11}$	$2.2417*10^{-10}$	$1.445*10^{-10}$
0.3	0.75	$7.13*10^{-12}$	$3.401*10^{-10}$	$7.386*10^{-10}$
	1.5	$9.62*10^{-12}$	$1.294*10^{-10}$	$1.907*10^{-10}$
	2.5	$1.1112*10^{-11}$	$1.72*10^{-10}$	$1.749*10^{-10}$

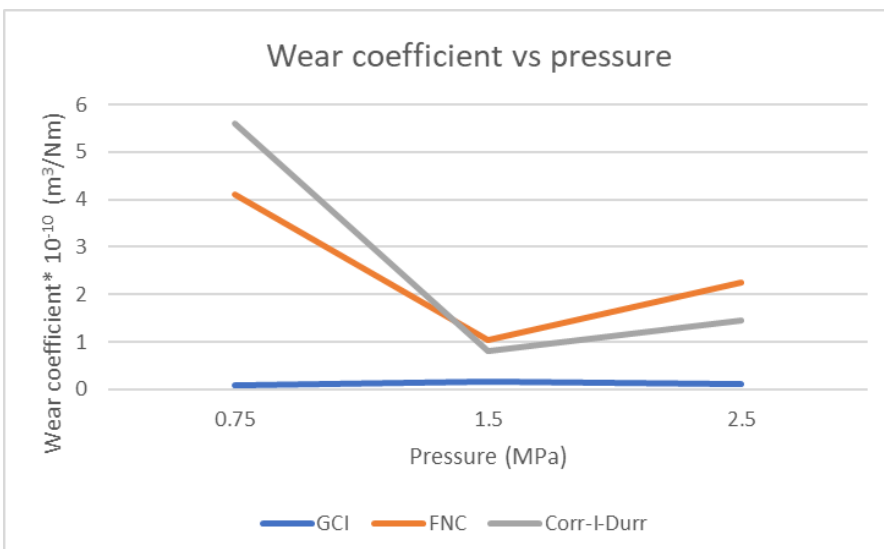

Figure 30: *Wear rate of the pad at 0.1m/s for treated and untreated brake discs*

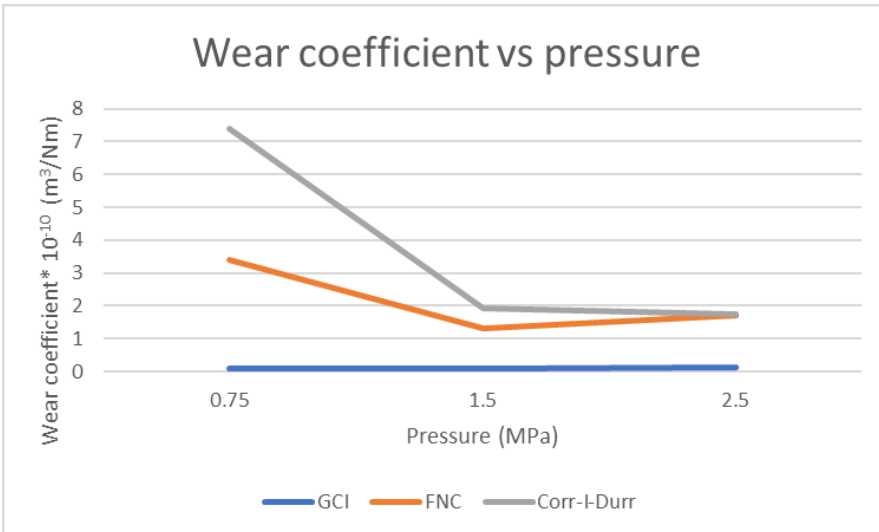

Figure 31: *Wear rate of the pad at 0.3m/s for treated and untreated brake discs*

Figure 31 and Figure 32 show that, for the constant velocity, the wear coefficient decreases when the pressure increase for the FNC-treated brake discs. For the higher pressure, the wear coefficient increases again. This trend looks similar for two different sliding velocities. In the case of untreated GCI, the wear coefficient increases when the pressure increases. The wear loss for the brake pads used for the untreated GCI brake discs is also low.

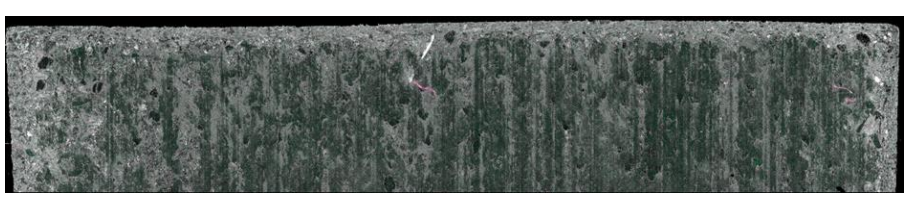

Figure 32: *A microscopic view of Tool 3 edge for Velocity 0.1m/s and 2.5MPa for FNC disc*

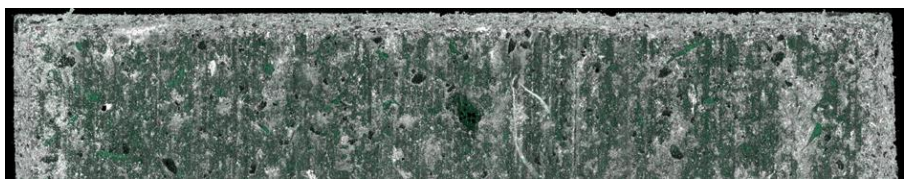

Figure 33: *A microscopic view of Tool 3 edge for Velocity 0.1m/s and 2.5MPa for FNC disc*

Figure 32 and Figure 33 represent the same tool used for two different conditions for the FNC brake discs. And it can be seen that the brake pads will be worn out if the pads are used continuously for a certain time and the high pressure. The wear loss of the brake pads can be related to the surface roughness and the surface hardness of the disc's materials.

Figure 34: *The photograph of the wear tracks of different brake discs for velocity 0.1m/s and 2.5MPa. a) GCI b) FNC and c) Corr-I-Durr discs*

Figure 34 reveals that FNC-treated brake discs generated more wear particles than the other brake discs under the same test conditions. Many loose particles from the brake pads are found on the surface of FNC- treated brake discs. And no cracks or fractures are visible in the three different brake discs.

5.5. Surface Roughness

A profilometer was used to analyze the surface roughness of the brake discs. The values obtained were carried out before experimenting in the tribotester machine. Ra value is the arithmetic mean deviation of the roughness profile.

Rz is the average maximum height of the profile, Rmax is the maximum roughness depth.

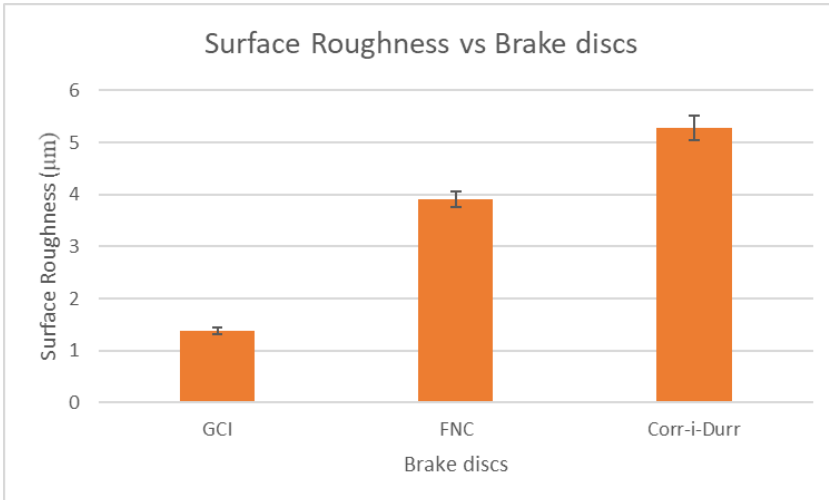

Figure 35: *Surface roughness of brake discs*

Figure 35 shows that Corr-I-Durr brake discs have higher surface roughness compared to the untreated GCI. This roughness is measured before the experiment. The roughness of the brake discs depends on the material constituents present and machining.

5.6. Chapter Summary

The chapter starts by explaining the microstructure of both GCI samples and FNC samples. The second part discusses the surface hardness of the brake discs. The later part of the chapter presents the results of the tribology test, which includes COF and wear, and the graphs are plotted. The last part explains the surface roughness and how it varies for FNC-treated and untreated GCI brake discs.

6. Discussions

This chapter analyses the results obtained during the experiments and supports theoretical literature, and the research questions were answered.

The FNC-treated brake discs can be considered an alternative solution for the GCI brake discs based on the COF and wear behavior. Mehdi Karim [62] observed that the compound layer is uniform throughout the surface and has a hardness range of 700-900HV. The results from this experiment are presented in Figure 22, which shows that the thickness of the compound layer is not uniform and varies in the range from 10 µm to 48 µm and pores visible on the compound layer. The microhardness measurement shows that FNC samples have a hardness range of 175-190 HV, which is low compared to the literature.

RQ1: What is the effect of sliding velocity and contact pressure on COF for the FNC treated and untreated brake discs?

The experiment was carried out for different pressure and velocities. FNC-treated brake discs show high COF increases initially and then start to decrease with an increase in pressure. This can be observed from the Huang et al., 2007 [46] theory, as the braking pressure affects the friction force mainly through the variations in the contact area. Figure 24 shows the same results in which the COF decrease when the pressure increase. This can be explained that the actual contact area between the pads and surface must have attained a stable value, and this contact area ratio was lower than the applied pressure, resulting in decreased COF.

Zhang 2003; [49] and Sviridenok and Meshkov 2005 [50] proved the COF will decrease when the sliding velocity increases. Figure 24- Figure 26 shows similar results; when the velocity is increased, the COF is decreased. This can be because of the increase in temperature, which leads to the formation of the tribofilm. Österle et al. [51] concluded that tribofilm is formed by the combination of plastic deformation, compaction, oxidation, and mechanical mixing of wear particles. When the tribofilm gets thicker, it starts to shear, which leads to a decrease in COF.

Initially, Figure 24-Figure 26 shows the higher increase in the COF for the first 10 passes. This is because less amount of wear-resistant material is removed from the pads, which leads to the direct contact of more resistant

material, typically reinforcing the ingredients of the pads to the brake discs, which causes the increase in the COF. This area of direct contact is called the primary plateau. Then, direct contact will grow when the surface subjects to the wear debris, forming the secondary plateau [48].

The experiment results in Figure 27 and Figure 28 show the mean COF of the FNC brake discs start to increase for the increase in the braking conditions like pressure and wear. This is because the newly produced brake discs will have the spiral ridge pattern resulting from the turning operation, and this will gradually wear off, which Kemmer observed [63].

The friction depends on the microstructure of the brake discs. The amount of graphite present in the GCI will influence an increased COF [52]. The friction also depends on the surface irregularities between the discs and pads. As the FNC treated, brake discs have higher surface roughness shown in Figure 35 compared to the untreated GCI. So the FNC-treated brake discs show a higher COF.

RQ2: what is the effect of sliding velocity and contact pressure on wear for the FNC treated and untreated brake discs?

The experiment results show that the brake discs' wear rate is also affected by sliding velocity and contact pressure. The wear of the brake discs is caused by the plastic deformation of the material in the contact surface. ML CHA [52] observes that the mechanical actions between the asperities become more with velocity increasing, the wear rate rises with the velocity in this period. It can be seen from Figure 30 and Figure 31 that for an increase in velocity, the specific wear rate of the brake discs also increases.

The compound layers contain the ε phase, which implies good wear resistance. The compound layer also provides wear resistance; the ceramic nature of the compound layer will provide low friction with material and prevent welding together [27]. But in this experiment, the brake pads used for the FNC brake discs show higher wear loss because the compound layer is thin and would have worn out at the initial stages. And when the braking conditions increased, the resistance towards abrasion is reduced drastically.

Wahlström [64] observed that lower initial surface roughness results in higher creation of the secondary plateaus. This is in line with the results, which can be seen in Figure 35. It shows that the surface roughness of the FNC-treated brake discs is higher than the untreated brake discs. FNC has

high surface roughness, and the brake pads used for the FNC brake discs are worn out more than untreated.

It can be observed from Figure 29, that brake pads used for FNC-treated brake discs show high wear loss compared to the ones used for the GCI brake discs. The brake pads show high wear loss for the first 100 passes because of the surface roughness of the material. An increase in the number passes with an increase in pressure, the wear loss of the pads decreases. This leads to the formation of the tribofilm and the presence of the compound layer. Further increase in passes will increase the temperature, and the tribofilm starts to shear off, and the compound layer is also worn out that increases the wear loss of the pads.

Wear tracks obtained from the experiment Figure 34 shows many loose particles are seen on the FNC-treated brake discs. The abrasive wear particles are visible on the FNC-treated brake discs, and it is higher than the untreated GCI disc surface. Also, no cracks or fractures were observed on both brake disc surfaces.

7. Conclusion

The aim of this study is to investigate the tribological behavior (Friction and wear) of FNC treated GCI brake discs and compared the results with the untreated GCI brake rotor. The results from the tribological experiments and the microstructure of these samples were analyzed and concluded.

1. The braking load and the sliding velocity have a higher effect on the friction coefficient. As the braking pressure increases, the friction coefficient increases. And when the sliding velocity increases, the temperature will increase, which decreases the friction coefficient.
2. The tribofilm formed during the experiment over the surface acts as a protective layer.
3. Similarly, the loading conditions affect the wear rate of the brake discs. The pressure increases, the wear rate starts to increase.
4. The FNC-treated GCI brake discs have a higher COF, about 0.27, than the untreated GCI, about 0.24.
5. FNC-treated GCI brake disc shows higher wear rate than the untreated GCI brake disc.
6. The Microhardness of the untreated GCI brake disc is high. Despite the thickness of the compound layer present in the FNC-treated GCI brake discs, it shows lower hardness.
7. The surface roughness of the FNC-treated GCI brake discs is high, which is the primary factor in determining the COF and wear rate.

The FNC surface-treated brake discs show high friction coefficient, but the wear rate for the brake discs is high. The thickness of the nitrocarburized compound layer determines the efficiency of the brake discs, and the compound layer is not uniform throughout the surface. As the brake pads show a high amount of weight loss when used for FNC brake discs, it will affect the braking performance. The experiments are carried out only for the 100 passes for each condition; increasing loading conditions and the number of passes can lead to different results. So it is suggested that untreated GCI is a better material for brake discs from the obtained result.

Recommendation for future study

The following recommendations were made based on the conclusions from this investigation. For future research, it is recommended to perform the studies by increasing contact pressure and sliding distance. The particles generated in the wear track during the experimentation can also be analyzed to understand the material properties better.

Future research can be performed to analyze the corrosion behavior of the FNC samples. The authors suggest smoothening the FNC brake disc surface by machining to reduce the surface roughness to get better results. The NAO brake pads are generally used for GCI brake discs, and if different brake pad materials were used for FNC, it might have shown different results.

8. Bibliography

[1] S. A. Awe, "Developing Material Requirements for Automotive Brake Disc," *Modern Concepts in Material Science,* vol. 2, 2019.

[2] R. Thornton, T. Slatter, A. Jones and R. Lewis, "The effects of cryogenic processing on the wear resistance of grey cast iron brake discs," *WEAR,* vol. 271, no. 9-10, pp. 2386-2395, 2011.

[3] N. Athanassiou, U. Olofsson, J. Wahlström and S. Dizdar, "Simulation of thermal and mechanicalperformance of laser cladded disc brake rotors," *Proceedings of the Institution of Mechanical Engineers, Part J: Journal of Engineering Tribology,* 2021.

[4] O. Aranke, W. Algenaid and S. A. a. S. Joshi, "Coatings for Automotive Gray Cast Iron Brake discs: A Review," 2019.

[5] O. Aranke, W. Algenaid, S. Awe and S. Joshi, "Coatings for Automotive Gray Cast Iron Brake Discs," *Coatings,* vol. 9, no. 9, p. 552, 2019.

[6] Saundrers, M. Lewis and A. Thornil, "Research Methods for Buisness Students," 2012.

[7] P. Coughlan and D. Coghlan, "Action Research for Operations Management.," *Internatinal Journals of Operations & Production Management,* vol. 22, 2002.

[8] A. Bryman and E. Bell, "Buisness Research Methods," 2011.

[9] J. Rowley and F. Slack, "Conducting a Literature Review," *Management Research News,* vol. 27, no. 6, pp. 31-39, 2004.

[10] S. Kabir, "Basic Guidelines For Research: An Introductory Approach For All Disciplines," Chittagong: Book Zone Publication, 2016, pp. 201-275.

[11] J. Wahlström, “A study of airborne wear particles from automotive disc brakes,” 2011.

[12] U. Olofsson, Y. Lyu, A. W. J. Hedlund Åström, S. Dizdar, A. P. Gomes Nogueira and S. Gialanella, “Laser cladding treatment for refurbishing disc brake rotors – environmental and tribological analysis,” 2021.

[13] S. Dizdar, Y. Lyu, C. Lampa and U. Olofsson, “Grey Cast Iron Brake Discs Laser Cladded with Nickel-Tungsten Carbide—Friction, Wear and Airborne Wear Particle Emission,” *Atmosphere,* vol. 11, no. 6, p. 621, 2020.

[14] F. G. Technologies, “Brake disk and method for producing brake disk,” 2020.

[15] G. Bolelli, V. Cannillo, L. Lusvarghi and T. Manfredini, “Wear behaviour of thermally sprayed ceramic oxide coatings,” *Wear,* vol. 261, no. 11-12, pp. 1298-1315, 2006.

[16] P. S. Babu, D. Sen, A. Jyothirmayi, L. R. Krishna and D. S. Rao, “Influence of microstructure on the wear and corrosion behavior of detonation sprayed Cr2O3-Al2O3 and plasma sprayed Cr2O3 coatings,” 2017.

[17] T. Sahraoui, N.-E. Fenineche, G. Montavon and C. Coddet, “Structure and wear behaviour of HVOF sprayed Cr3C2–NiCr and WC–Co coatings,” 2003.

[18] D. Toma, W. Brandl and G. Marginean, “Wear and corrosion behaviour of thermally sprayed cermet coatings,” *Surface and Coatings Technology,* vol. 138, no. 2-3, pp. 149-158, 2001.

[19] I. Hulka, V. Şerban, I. Secoşa, P. V. and K. Niemi, “Wear properties of CrC–37WC–18M coatings deposited by HVOF and HVAFspraying processes,” *Surface & Coating Technology,* 2012.

[20] Rajasekeran, Theisen, Vassen, W. S and Röttger, “Mechanical properties of thermally sprayed Fe based coatings. Mater. Sci. Technolgy,” pp. 973-982, 2011.

[21] G. Bolelli, T. Börner, A. Milanti, L. Lusvarghi, J. Lauril and H. Koivuluoto, “Tribological behavior of HVOF- and HVAF-sprayed composite coatings based on Fe-Alloy + WC–12% Co,” 2014.

[22] P. Sassatelli, G. Bolelli, L. Lusvarghi, T. Manfredini and a. R. Rigon, “Manufacturing and Properties of HighVelocity Oxygen Fuel (HVOF)-Sprayed FeVCrC Coatings,” 2016.

[23] MCcan and Jake, “Advance Heat Treatment Corporation”.

[24] T. Holm and L. Sproge, “Nitriding and Nitrocarburizing”.

[25] Nan and Chunyan, “Ferritic Nitrocarburizing Process Development for minimization of distortion,” 2009.

[26] D. Pye, “Nitriding Techniques,” pp. 531-537.

[27] I. FLODSTRÖM, “Nitrocarburizing and High Temperature nitriding of steel and applications”.

[28] M. A. Fontesa, R. G. Pereirab and Frederico Augusto Pires Fernandesb, “Characterisation of Plasma nitrided layers produced on sintered iron,” 2014.

[29] M. A. J. Somers, “Thermodynamics, kinetics and microstructural evolution of the compound layer,” *Heat Treatment of Metals* , pp. 92-100, 2000.

[30] M. k. Zarchi, M. H. Sharait and S. A. Dehghan, “Characterization of nitrocarburized surface layer on AISI 1020 steel by electrolytic plasma processing in an urea electrolyte,” *Journal of materials Research and Technology,* 2013.

[31] M. Fattah and F. Mahboubi, “Comparison of Ferritic and Austentic Plasma Nitriding and nitrocarburized behaviour of AISI 4140 low alloy steel,” *Materials and Design,* vol. 30, pp. 3915-3921, 2010.

[32] L.Wei and Y. a. C.S.Cheung, “A study of brake contact pairs under different friction conditions with respect to characteristics of brake pad surfaces,” vol. 138, pp. 99-110, 2019.

[33] P. G. Sanders, N. Xu, T. M. Dalka and a. M. M. Maricq, “Airborne Brake Wear Debris: Size Distributions, Composition, and a Comparison of Dynamometer and Vehicle Tests,” 2003.

[34] K.Jain and M. K. S. a. Vinod, “Friction and wear characteristics of hard coatings,” vol. 251, no. 1-12, pp. 990-996, 2001.

[35] G. W.Stachowiak, A. W.Batchelor and G. B.Stachowiak, Experimental Methods in Tribology (Tribology series), Elsevier Science Limited, 2004.

[36] Byrom and T. G., Casing and Liners for Drilling and Completion, 2015.

[37] Qatu and P. Mohamad, “Vehicle Noise and Vibration,” vol. 10, p. 4, 2014.

[38] Carpick and C. M. M. a. R. W., Tribology on the Small Scale: A Modern Textbook on Friction, Lubrication, and Wear$, Oxford Scholarship, 2019.

[39] M. Varenberg, “Towards a unified classification of wear,” 2013.

[40] H. Kemmer, “Investigation of the Friction Behavior of Automotive Brakes Through Experiments and Tribological Modeling,” 2002.

[41] W. Österle and A. Dmitriev, “Functionality of conventional brake friction materials - perceptions from findings observed at different length scales.,” *Wear,* vol. 271, no. 9-10, pp. 2198-2207, 2011.

[42] W. Osterele, I.Dorfel, C.Prietzel and A. H.Rooch, “A comprehensive microscopic study of third body formation at the interface between a brake pad and disc during the final stage of pin on disc.,” *Wear,* pp. 781-789, 2009.

[43] Urban and W. Österle, “Third body formation on brake pads and rotors,” *Tribology International,* pp. 401-408, 2006.

[44] H. Jang, K. Ko, S. Kim, R. Basch and J. Fash, “The effect of metal fibers on the friction performance of automotive brake friction materials,” vol. 256, no. 3-4, pp. 406-414, 2004.

[45] Y. Yin, J. Bao and L. Yang, “Frictional performance of semimetal brake lining for automobiles,” *Industrial Lubrication and Technology,* pp. 33-38, 2012.

[46] P. Huang, Y. Meng and H. Xu, “Tribology Course,” 2007.

[47] M. Eriksson, F. Bergman and S. Jacobson, “On the nature of tribological contact in automotive brakes.,” *Wear,* pp. 26-36, 2002.

[48] J. Wahlström, V. Matějka, Y. Lyu and A. Söderberg, “Contact Pressure and Sliding Velocity Maps of the Friction, Wear and Emission from a Low-Metallic/Cast-Iron Disc Brake Contact Pair,” *Tribology in Industry,* pp. 460-470, 2017.

[49] X. Zhang, “Study of carbon fiber reinforced automotive friction materials,” *Automobile Technology and Materials,* vol. 18, pp. 9-11, 2003.

[50] A. Sviridenok and V. and Meshkov, ““High-speed sliding friction of polymer composites”,” *Journal of Friction and Wear,* vol. 26, 2005.

[51] W. Österle and a. A. Dmitriev, “Functionality of conventional brake frictional materials; Perceptions from findings observed at different length scales,” *Wear,* vol. 271, pp. 2198-2207, 2011.

[52] M. Cho, S. Kim, R. Basch, J.W, Fash and H. Jang, “Tribological study of gray cast iron with automotive brake linings:The effect of rotor microstructure,” *Tribology International,* pp. 537-545, 2003.

[53] A. Rehman, S.Das and G.Dixit, “Analysis of stir die cast Al–SiCcomposite brake drums based on coefficient of friction,” *Tribology International,* 36-41.

[54] S. Ananth, J. U. Prakash, R. K. Murthy, K. V. A. Pillai and T. V. Moorthy, "Tribological Behaviour of Grey Cast Iron–EN31 Steel Contact Under Sliding Conditions," 2020.

[55] C. K, S. N and a. D. R, "Tribology," 2013.

[56] Y. Yin, J. Bao and L. Yang, "Wear performance and its online monitoring of the semimetal brake lining for automobiles," *Industrial Lubrication and Tibology,* vol. 66, no. 1, pp. 100-105, 2014.

[57] L. Kirkhorna, K. Frognera, M. Andersson and J. Ståh, "Improved Tribotesting for Sheet Metal Forming," p. 6, 2021.

[58] "Focus-Variation," [Online]. Available: https://www.alicona.com/our-technology/focus-variation/. [Accessed 2021].

[59] "Scanning Electron Microscope (SEM)," Bioscience Notes, 18 june 2018. [Online]. Available: https://www.biosciencenotes.com/scanning-electron-microscope-sem/. [Accessed 2021].

[60] K. Subramanian, G. Janavi, S.Marimuthi, M.Kannan, K.Raja, S. Haripriya, D. S. Sharimili and P. Moorthy, FUNDAMENTALS AND APPLICATIONS OF NANOTECHNOLOGY, 2018.

[61] "An Introduction to Electron Microscopy for Biologists," Bitesize Bio, 9 july 2016. [Online]. Available: https://bitesizebio.com/29197/introduction-electron-microscopy-biologists/. [Accessed 2021].

[62] M. Karimi Zarchi, M. H. Shariat, S. A. Dehghan and S. Solhjoo, "Characterization of nitrocarburized surface layer on AISI 1020 steel by electrolytic plasma processing in an urea electrolyte," *Journals of Material Research and Technology,* 2013.

[63] H.A.Kemmer, "Investigation of the Friction Behavior of Automotive Brakes through experiments and Tribological Modeling," 2002.

[64] G. Riva, G. Perricone and J. Wahlström, “Simulation of Contact Area and Pressure Dependence of Initial Surface Roughness for Cermet-Coated Discs Used in Disc Brakes,” *Tribology in Industry,* vol. 41, no. 1, pp. 1-13, 2019.

Appendix

Hardness

Table 1: The table showing the Vickers Hardness values for different trails for the three different samples.

Trial	CGI	FNC	Corr-I-Durr
1	197.7	192.4	175.7
2	209	171.1	166.2
3	192.1	196.8	187.9
4	187	192	184.3
5	199.9	183.6	175.5
6	203.7	172.6	162
7	202.6	181.2	164.6
8	207	177.7	189
AVERAGE	199.8	183.425	175.65
Standard Deviation	±6.955	±8.942	±10.005

Surface Roughness

Table 2: Showing the surface characteristics of GCI brake discs

	Ra (μm)	Rz(μm)	Rmax(μm)	L_T (mm)
Trail 1	1.443	9.67	19.6	5.6
Trail 2	1.554	11.5	11.5	5.6
Trail 3	1.173	12.9	12.9	5.6
Trail 4	1.352	11.6	11.6	5.6

Table 3: Showing the surface characteristics of FNC brake discs

	Ra (µm)	Rz (µm)	Rmax (µm)	L_T (mm)
Trail 1	3.625	21.0	28.3	5.6
Trail 2	3.690	26.4	39.8	5.6
Trail 3	4.365	21.3	27	5.6
Trail 4	3.975	28.8	41.2	5.6

Table 4: Showing the surface characteristics of Corr-I-Durr brake discs

	Ra (µm)	Rz (µm)	Rmax (µm)	L_T (mm)
Trail 1	5.995	34.2	52.7	5.6
Trail 2	5.4	40.2	63.0	5.6
Trail 3	5.008	29.6	56.1	5.6
Trail 4	4.734	30	39.9	5.6

Coefficient of friction

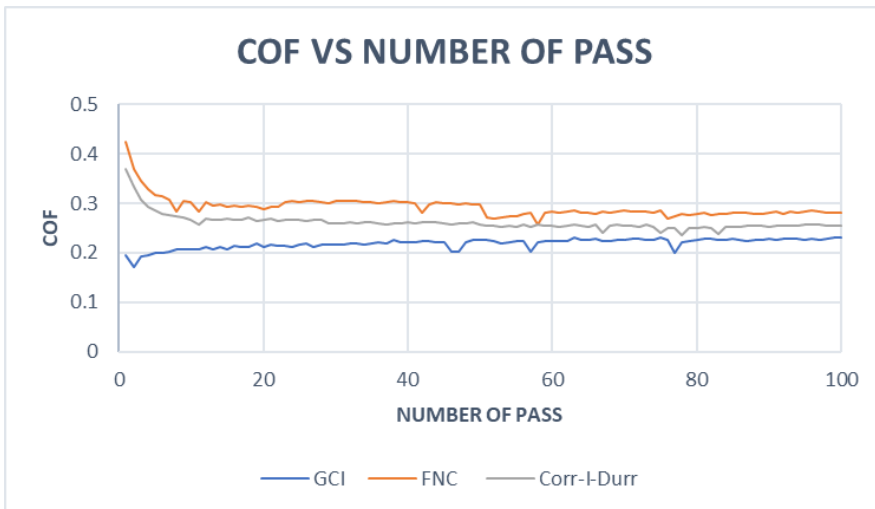

Figure 1: Coefficient of friction vs. number of pass for velocity 0.1m/s and 0.75MPa

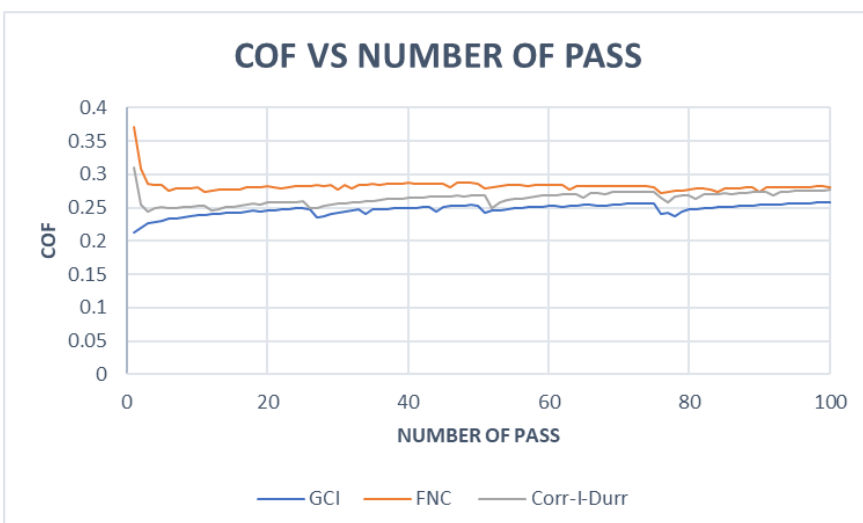

Figure 2: Coefficient of friction vs. number of pass for velocity 0.1m/s and 2.5MPa

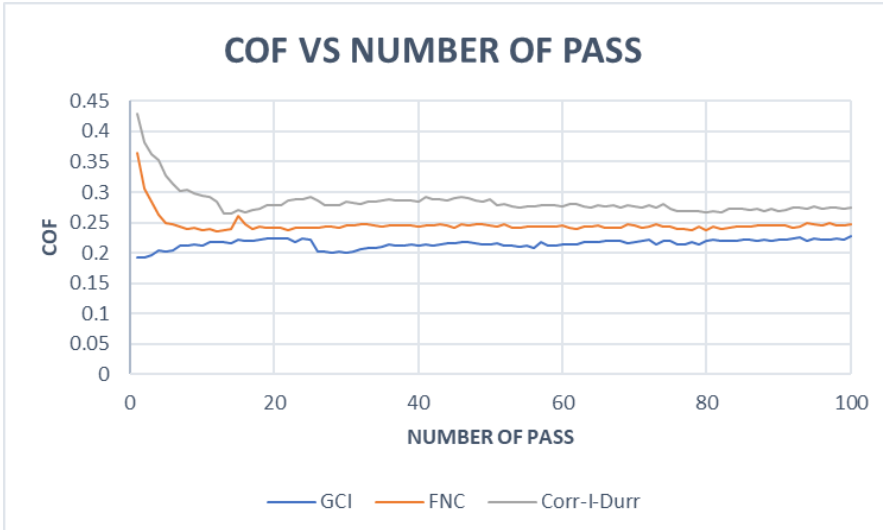

Figure 3: Coefficient of friction vs. number of pass for velocity 0.3m/s and 2.5MPa